Alzheimer's disease (AD) is the most prevalent cause of dementia and is characterized by loss of memory and cognition as well as behavioral and occupational instability in old age. One of the pathological characteristics of AD is the progressive deposition of insoluble amyloid β protein (Aβ) as a form of senile plaques (Wirths *et al.* 2004). This protein comprises peptides of approximately 39 to 43 amino acid residues derived from the transmembrane amyloid precursor protein (APP) (Selkoe 2002). Aβ can form monomers and a variety of different aggregate morphologies including dimers, small soluble oligomers, protofibrils, diffuse plaques, and fibrillar deposits seen in the senile plaques. Protofibrils, diffuse plaques, and fibrillar deposits seem to have a predominant β-sheet structure (Tierney *et al.* 1988; Barrow and Zagorski 1991), while oligomers are believed to be more globular (Barghorn *et al.* 2005). Increasing evidence that the formation of these aggregates, particularly oligomer, causes primary neurodegeneration in AD has led to the amyloid hypothesis which states that the accumulation of Aβ in the CNS is highly neurotoxic and deteriorates synaptic functions (Selkoe 2002; Wirths *et al.* 2004). Moreover, several lines of evidence suggest that Aβ accumulation begins at relatively early stages before cognitive decline becomes manifest (Anderton *et al.* 1998; Selkoe 2002). Therefore, it is hypothesized that the formation, deposition, and aggregation of Aβ in the brain should be primary targets for complete amelioration of dementia. Currently, drugs available for dementia such as acetylcholinesterase inhibitors exert only a temporary benefit on cognitive dysfunction (Millard and Broomfield 1995; Park *et al.* 2000; Darreh-Shori *et al.* 2004), and they do not prevent or reverse the formation of Aβ deposits. One potentially promising strategy for developing more effective anti-dementia drugs is the inhibition of Aβ fibril formation or destabilization of aggregated Aβ or a combination of both.

Herbal remedies are used worldwide and have a long history of use in alleviating a variety of symptoms of many different conditions and diseases. Recently, clinical trials in AD patients have also shown that some of these traditional medications improved Mini-Mental State Examination scores, P300 latency, and blood flow in the cerebral cortex (Le Bars *et al.* 1997). Although inconclusive, these provocative studies suggest that even old remedies can be beneficial in AD and related disorders. We have reported that several traditional herbal medicines such as *Formula lienalis angelicae compositae* (kamiuntanto) (Suzuki *et al.* 2001; Nakagawasai *et al.* 2004), *Pilulae octo-medicamentorum rehmanniae* (hachimijiogan) (Iwasaki *et al.* 2004), and *Pulvis depressionis hepatis* (yokukansan) (Iwasaki *et al.* 2005) improved symptoms of dementia. The radicis cortex of *Paeonia suffruticosa* (*Moutan cortex*; Botan-pi), a major medicinal plant comprising *Pilulae octo-medicamentorum rehmanniae*, is used as an anti-pyretic and anti-inflammatory agent (Lin *et al.* 1999; Yasuda *et al.* 1999; Chou 2003). Paeonol, a common component of *Paeonia suffruticosa*, has been shown to inhibit platelet aggregation in rabbits (Lin *et al.* 1999) as well as to reduce cerebral infarction in ischemia-reperfusion-injured rats (Hsieh *et al.* 2006). However, the underlying mechanism of traditional medicinal herbs, including *Paeonia suffruticosa*, on the formation and metabolism of Aβ fibrils has never been investigated. In the present study, we examined the effect of *Paeonia suffruticosa* on the formation of Aβ aggregates and its ability to destabilize pre-formed Aβ fibrils *in vitro* by using fluorescence spectroscopy with thioflavin T.

1,2,3,4,6-Penta-*O*-galloyl-β-D-glucopyranose (PGG), a high molecular weight tannin-type polyphenols, has been isolated from *Paeonia suffruticosa*. The defining characteristic of tannins is their ability to bind and precipitate proteins (Hofmann *et al.* 2006). Li *et al.* (2005) previously reported that PGG could bind to insulin receptors and activate an insulin-mediated glucose transport signaling pathway. However, the effect of this compound on the formation and metabolism of Aβ fibrils has not yet been investigated.

Our results provide strong evidence that several traditional herbs extracts including *Paeonia suffruticosa* and PGG have inhibitory and destabilizing effects on Aβ fibrils.

Materials and methods

Reagents

Aβ peptides (1–40 and 1–42) and thioflavin-T were obtained from Peptide Institute (Osaka, Japan) and from Sigma (St Louis, MO, USA), respectively. All the reagents and drugs used were of analytical grade.

Preparation of medicinal herb extracts

Water, 100% methanol, and 99.5% ethanol extracts of medicinal herbs were prepared by refluxing 10 g of sliced dry herbs in 100 mL of each solution for 30 min. The decoction after cooling to 25°C was evaporated completely under reduced pressure to yield dried or oily extracts. The extracts were weighed and dissolved in dimethylsulfoxide at a concentration of 100 mg/mL and then stored at −20°C. When assaying, these extracts were dissolved in 50 mM potassium phosphate buffer (pH 7.4) and the solutions were adjusted to pH 7.4 when necessary.

Analysis of three-dimensional HPLC fingerprints of water extract of *Paeonia suffruticosa*

Paeonia suffruticosa (0.5 g) was extracted with 30 mL of distilled water under ultrasonication for 30 min. The solution was filtered and then analyzed by HPLC. The HPLC system consisted of an HPLC pump (LC-10AD; Shimadzu, Kyoto, Japan) and a TSK-GEL 80_{TS} column (4.6 mm × 250 mm), and (A) 50 mM acetic acid-ammonium acetate and (B) acetonitrile were used as the eluents. A linear gradient of 90% A and 10% B changing over 60 min to 0% A and 100% B was used. The flow rate was controlled at 1.0 mL/min. After the eluate was obtained from the column, the three-dimensional data were processed with a diode array detector (SPD-M10A; Shimadzu).

Thioflavin-T measurement

Thioflavin-T measurement was performed using the method described by Suemoto *et al.* (2004) with slight modifications. For the Aβ aggregate-formation assay, Aβ (20 μM) dissolved in the 50 mM potassium phosphate buffer (pH 7.4) with a test herbal extract was incubated at 37°C for 96 h ($A\beta_{1-40}$) or 24 h ($A\beta_{1-42}$). For the destabilization assay of pre-formed Aβ aggregates, after incubation of $A\beta_{1-40}$ (96 h) or $A\beta_{1-42}$ (24 h) without a test herbal extract, a mixture of the aggregated Aβ and a test herbal extract was incubated for 30 min at 37°C.

At the end of the incubation, 3 μM thioflavin-T dissolved in 100 mM glycine buffer (pH 8.5) was added to the mixture. Fluorescence of thioflavin-T bound to Aβ aggregates was measured using a microplate reader (Spectramax GEMINI XS; Molecular Devices, Sunnyvale, CA, USA) (excitation at 442 nm and emission at 485 nm) after incubation for 30 min at 25°C. The percentage inhibition was calculated by comparing the fluorescence values of test samples with those of control solutions without herbal extracts.

Animals

Tg2576 APPswe mice over-express a 695-amino acid splice form (Swedish mutation K670N M671I) of the human Aβ precursor protein (APP695) which resulted in a fivefold increase in $A\beta_{1-40}$ and a 14-fold increase in $A\beta_{1-42}$ with increasing age, driven by the hamster prion protein promoter. The animals were allowed free access to water and standard laboratory food in a facility with the temperature controlled at 24 ± 1°C and relative humidity at 55 ± 5%, with lights on from 7:00 to 19:00 hours daily. Behavioral studies were performed between 10:00 and 12:00 hours. Experimental protocols were approved by the Animal Care and Use Committee, Tohoku University Graduate School of Medicine, and complied with the procedures outlined in the Guide for the Care and Use of Laboratory Animals of Tohoku University.

Step-through passive-avoidance test

The apparatus (AP model; O'Hara Co., Tokyo, Japan) for the step-through passive-avoidance test consisted of two compartments, illuminated compartment [100 mm × 120 mm × 100 mm; light at the top of compartment (27W, 3000 lx)] and dark compartment (100 mm × 170 mm × 100 mm). The compartments were separated by a guillotine door. During the learning stage, a mouse was placed in the illuminated safe compartment. As the compartment was lit, the mouse stepped through the opened guillotine door into the dark compartment. The time spent in the illuminated compartment was defined as the latency time. Three seconds after the mouse entered the dark compartment, a foot shock (0.3 mA, 50V, 50 Hz ac, for 3 s) was delivered to the floor grids in the dark compartment. The mouse could escape from the shock only by stepping back to the safe illuminated compartment. Such acquisition trials during the learning stage were carried out once a day for 5 days. It was judged as learning avoidance from foot-shock if the mouse remained in the illuminated compartment for 300 s after being placed there. The retention trials were carried out once per week for 10 weeks from Days 8 to 78 to evaluate the retention of avoidance memory. The latency time was measured for up to 300 s without delivering foot-shock. It was judged that the mouse retained the avoidance memory when it stayed in the illuminated safe compartment for 300 s. Acquisition and retention trials were conducted in 11-month-old mice.

Immunocytochemistry

All sample brains were fixed in neutral-buffered formalin and embedded in paraffin. Immunocytochemistry was performed using an Amyloid β Protein Immunohistostain Kit (Wako Pure Chemical Industries, Ltd., Osaka, Japan) according to the manufacturer's instructions. Briefly, after deparaffinization, 8-μm brain sections were immersed in 99% formic acid for 5 min, blocked with blocking serum, and immunostained with BA27 ($A\beta_{1-40}$) and BC05 ($A\beta_{1-42}$) by a standard avidin–biotin complex method, using 3,3′-diaminobenzidine as chromogen and lightly counter-staining with hematoxylin.

Tissue preparation

Tissue samples were processed in Tris-buffered saline (soluble fraction) and 70% formic acid (insoluble fraction) containing 1× protease inhibitor mixtures as described previously (Calon *et al.* 2004) with slight modifications. Briefly, brain tissues were homogenized and sonicated in Tris-buffered saline containing protease inhibitor mixture. The resulting homogenate was subjected to ultracentrifugation at 200 000 *g* at 4°C for 20 min, and the soluble supernatant was collected and frozen. To analyze the insoluble Aβ, the insoluble pellet was sonicated in 200 μL of 70% formic acid and subjected to ultracentrifugation at 300 000 *g* at 4°C for 30 min, and the soluble supernatant was collected.

Aβ levels

Brain $A\beta_{1-40}$ and $A\beta_{1-42}$ levels were measured using sandwich ELISA with a Human β Amyloid ELISA Kit (Wako Pure Chemical Industries, Ltd.) according to the manufacturer's instructions. BAN50 is a monoclonal antibody raised against a synthetic peptide of human $A\beta_{1-16}$; it preferentially reacts with the N-terminal portion of human Aβ starting at Asp-1 but does not cross-react with N-terminally truncated Aβ nor with rodent-type Aβ. BA27 and BC05, which specifically recognize the C terminus of $A\beta_{1-40}$ and $A\beta_{1-42}$, respectively, were conjugated with horseradish peroxidase and used as detector antibodies. Mice brain insoluble fractions described above were neutralized and subjected to BAN50/BA27 or BAN50/BC05 ELISA. The amount of Aβ was calculated by comparing these absorbance values with those of control solutions without herbal extract.

Aβ ologomerization analysis

Amount of $A\beta_{1-42}$ oligomer was measured using Aβ Aggregate Human Singleplex Bead Kit (Invitrogen Corporation, Carlsbad, CA, USA) according to the manufacturer's instructions. Data analysis was performed by a flow cytometer (FACSCaliber, Becton Dickinson Immunocytometry Systems, Franklin Lakes, NJ, USA).

Cell viability assay

SK-N-SH cells were maintained in Dulbecco's modified Eagle's medium (Gibco Life Technologies, Carlsbad, CA, USA) supplemented with 10% fetal calf serum and 4 mM L-glutamine in a humidified atmosphere of 5% CO_2 and 95% air. SK-N-SH cells were seeded in 96-well plates at a density of 1×10^4 cells per well. After 24 h, we pre-incubated SK-N-SH cells for 30 min with PGG, followed by 24 h treatment with 10 μM aggregated $A\beta_{1-42}$. Cell

viability was assessed using the 3-(4,5-dimethylthiazol-2-yl)-2,5-diphenyltetrazolium bromide (MTT) method. Absorbance values of formazan were determined at 590 nm with an automatic microplate reader.

Data analysis

Data were expressed as mean ± SD. Statistical comparisons were made using ANOVA with Bonferroni's *post hoc* analysis. $p < 0.05$ was considered to be significant.

Results

Concentration-dependent effects of *Paeonia suffruticosa* on kinetics of Aβ fibril formation and breakdown

In our previous publication, it was noted that several medicinal herbs including *Uncaria rhynchophylla*, *Cinnamomum cassia*, and *Paeonia suffruticosa* showed destabilizing activity on Aβ fibrils (Fujiwara *et al.* 2006). *Paeonia suffruticosa* which was extracted either by water, methanol, or ethanol was concentrated under reduced pressure to yield oily residues (2.33, 1.89, and 2.14 g for water, methanol, and ethanol, respectively). To examine the inhibitory effect of *Paeonia suffruticosa* on Aβ fibril formation, concentration-dependencies were examined by the thioflavin T method. We observed that fluorescence intensity in $A\beta_{1-40}$ and $A\beta_{1-42}$ declined in a concentration-dependent manner (Fig. 1a and b). $A\beta_{1-40}$ fibril formation was inhibited by 10 μg/mL of the water (48.5 ± 0.3%), methanol (40.1 ± 2.8%), and ethanol (34.6 ± 0.2%) extracts of *Paeonia suffruticosa*. $A\beta_{1-42}$ fibril formation was also inhibited by each of the three different extracts (10 μg/mL), although the inhibitory concentration was lower than for $A\beta_{1-40}$.

In the analysis of fibril destabilization, fluorescence derived from thioflavin T was decreased in a dose-dependent manner after the addition of each of the extracts of *Paeonia suffruticosa* to pre-formed Aβ fibrils, and the degree of inhibition was similar to that observed on Aβ aggregation (Fig. 1c and d). Pre-formed $A\beta_{1-40}$ fibrils were destabilized by 10 μg/mL of the water (58.2 ± 3.7%), methanol (74.9 ± 1.1%) and ethanol (71.7 ± 1.0%) extracts. Over 80% of pre-formed $A\beta_{1-40}$ and $A\beta_{1-42}$ fibrils were destabilized by each of the three different extracts at the concentration of 100 μg/mL.

Step-through passive-avoidance tests

Step-through passive-avoidance tests were carried out in Tg2576 mice at 11 to 14 months of age. In the first acquisition trial of the learning stage, all mice (11 months

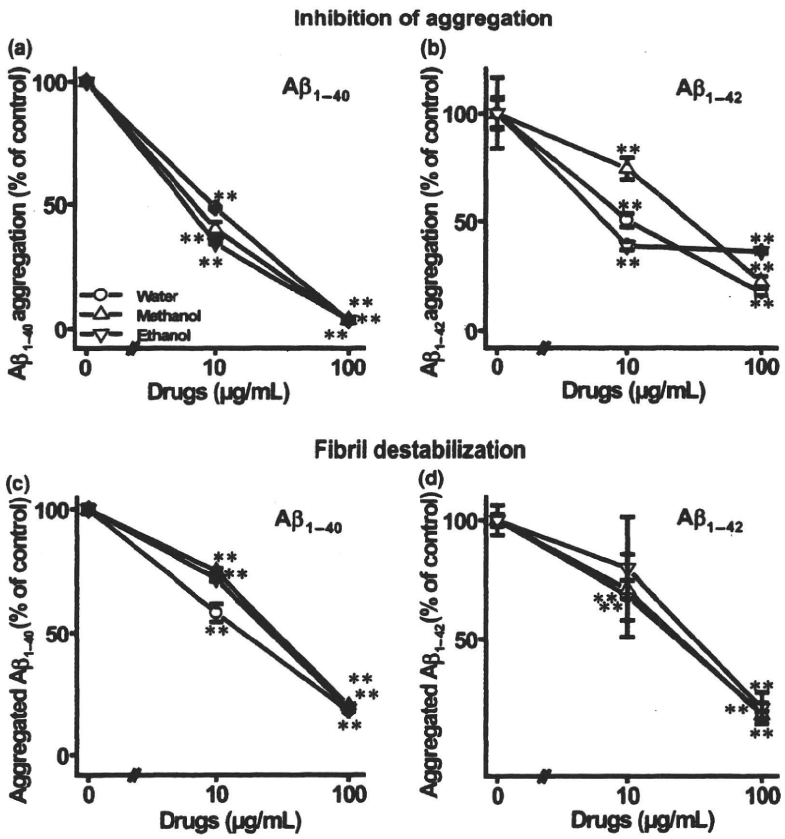

Fig. 1 Effects of three different *Paeonia suffruticosa* extracts on the kinetics of Aβ formation and destabilization. a and b: Aβ aggregate-formation assay. Reaction mixtures containing 20 μM of $A\beta_{1-40}$ (a) or $A\beta_{1-42}$, (b) 50 mM phosphate buffer (pH 7.4), and various extracts [water (circles), methanol (upward-pointing triangles), and ethanol (downward-pointing triangles)] were incubated at 37°C for 96 h (a) or 24 h (b). Aβ aggregation was expressed as percentage of the control sample which did not contain herbal extract. c and d: Aβ aggregate-destabilization assay. Reaction mixtures containing 20 μM $A\beta_{1-40}$ (c) or $A\beta_{1-42}$ (d) were incubated at 37°C for 96 h (c) or 24 h (d). The extracts were then added and incubated for another 30 min. Aβ aggregation was assessed by the thioflavin T method and expressed as the percentage of control aggregation in the absence of herbal extract. Values represent mean ± SD from four independent experiments. $^{**}p < 0.01$ compared with extract-untreated control.

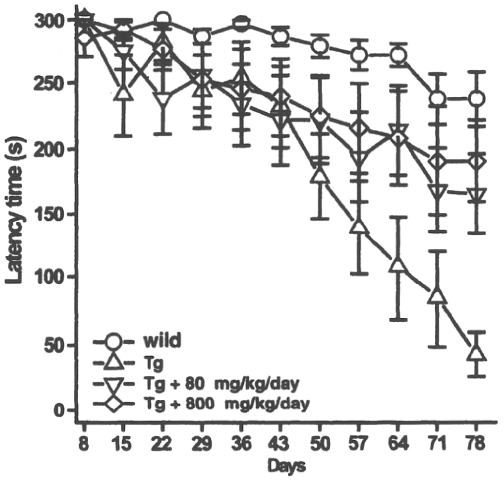

Fig. 2 Step-through latencies in the retention stages of the passive-avoidance task in *Paeonia suffruticosa*-treated transgenic (Tg2576) mice. Wild type and transgenic mice could acquire the avoidance memory by four or five repeated learning trials. The retention trials were carried out once per week for 10 weeks from Days 8 to 78 to evaluate the retention of avoidance memory. The latency time was measured for up to 300 s without delivering foot-shock. Wild type (Wild: circles); transgenic mice (Tg: upward-pointing triangles); 80 mg/kg/day *Paeonia suffruticosa* by repeated oral administration (Tg + 80 mg/kg/day: downward-pointing triangles), and 800 mg/kg/day *Paeonia suffruticosa* (Tg + 800 mg/kg/day: diamond). Values represent the means ± SD from 11 to 17 independent experiments.

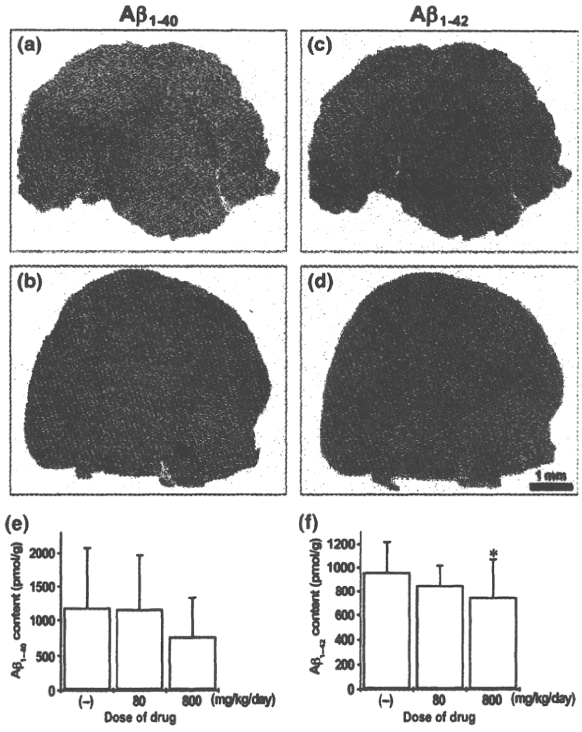

Fig. 3 Immunostaining (a–d) and ELISA analysis of formic acid-extractable Aβ levels (e and f) after dietary intake of *Paeonia suffruticosa* in Tg2576 mice. (a–d) Hemibrain cryostat sections were labeled with anti-$A\beta_{1-40}$ (a and b) and $A\beta_{1-42}$ (c and d) antibody. Image analysis was performed on the cerebral cortex from untreated (a and c) and *Paeonia suffruticosa*-treated (b and d) animals. Scale bar = 1 mm. Levels of $A\beta_{1-40}$ (e) and $A\beta_{1-42}$ (f) were quantified using an ELISA kit on formic acid-extractable Aβ from cortices of the low intake group (80 mg/kg/day) and high intake group (800 mg/kg/day). Values represent mean ± SD from 11 to 17 independent experiments. $^*p < 0.05$ compared with *Paeonia suffruticosa*-untreated control.

old) in the wild type and Tg groups entered the dark compartment immediately after being placed in the illuminated compartment. Repeating the acquisition trial increased the latency times in both groups. All mice in the wild type and Tg groups acquired avoidance memory, staying in the illuminated compartment for over 300 s on the fifth acquisition day. However, no significant differences were observed in the mean latency times between the wild type and Tg groups on any given day during the learning stage (data not shown). In retention trials (Fig. 2), the step-through latency of the Tg group was significantly reduced when compared with that of the wild type group. *Paeonia suffruticosa*-treated Tg mice were indistinguishable from non-transgenic littermates on days from 50 to 78 of testing.

Aβ pathology was reduced in *Paeonia suffruticosa*-treated Tg mice

To determine whether oral *Paeonia suffruticosa* treatment affected the accumulation of Aβ in brain tissue, we evaluated Aβ immunoreactivity in brain sections from untreated (Fig. 3a and c) and *Paeonia suffruticosa*-treated mice (Fig. 3b and d) using BA27 and BC05 antibodies which recognize the C-terminus of human $A\beta_{1-40}$ (Fig. 3a and b) and $A\beta_{1-42}$ (Fig. 3c and d). The number of Aβ-positive spots in the cortex and hippocampus were obviously lower in the *Paeonia suffruticosa*-treated mice compared with the untreated mice. No Aβ immunoreactivity was observed in brain sections from non-transgenic mice (data not shown).

We next measured the levels of $A\beta_{1-40}$ and $A\beta_{1-42}$ in brain tissue samples from Tg mice using a sensitive ELISA method (Fig. 3e and f). Consistent with the results of Aβ immunostaining, the $A\beta_{1-42}$ concentration in the samples from *Paeonia suffruticosa*-treated Tg mice (800 mg/kg/day) was significantly lower than the concentration in *Paeonia suffruticosa*-untreated mice (747.8 ± 322.4%, $p < 0.05$). In contrast to its effect on $A\beta_{1-42}$ levels, *Paeonia suffruticosa* treatment had no significant effect on $A\beta_{1-40}$ levels in the Tg mice. The levels of $A\beta_{1-40}$ and $A\beta_{1-42}$ were below the limit of detection in cerebral cortex samples from non-transgenic mice (data not shown).

HPLC analyses of *Paeonia suffruticosa*: identification of four different natural compounds and their effects on the kinetics of $A\beta_{1-42}$ formation and destabilization

The three-dimensional-HPLC fingerprints of water extracts of *Paeonia suffruticosa* are illustrated in Fig. 4. The water extract contained several different chemical compounds including paeonol, benzoic acid, and derivatives of paeoniflorin as well as PGG.

Concentration dependence of the inhibitory effects of these compounds on Aβ fibril formation was examined using the thioflavin T method (Fig. 5a). Only PGG induced a concentration-dependent decline in the thioflavin T fluorescence intensity associated with $A\beta_{1-42}$. PGG (3 μM) inhibited $A\beta_{1-42}$ fibril formation by more than 50%. Additional thioflavin-T experiments were performed in order to determine the ability of PGG to destabilize pre-formed Aβ fibrils. Fluorescence derived from thioflavin T was decreased in a dose-dependent manner after the addition of PGG to preformed Aβ fibrils to an extent similar to that seen for the inhibition of Aβ aggregation (Fig. 5b).

Next, we incubated different concentrations of PGG with unpolymerized $A\beta_{1-42}$ (10 μM) and monitored the formation of amyloid using the Thioflavin T method (Fig. 6). In the absence of PGG, $A\beta_{1-42}$ formed Thioflavin T-binding aggregates after a lag phase of 2 h, whereas thioflavin T signals were decreased to 33.6 ± 16.8% by 1 μM PGG after a lag phase of 24 h. Moreover, $A\beta_{1-42}$ aggregation was completely inhibited by 100 μM PGG.

Effect of PGG on $A\beta_{1-42}$ oligomers

To further characterize the breakdown products that accumulated in the presence of PGG, aliquots of $A\beta_{1-42}$ oligomerization reaction mixtures in the presence or absence of PGG were assayed by flow cytometric analysis (Fig. 7). In the absence of PGG, the fluorescence intensity of $A\beta_{1-42}$ oligomerized sample was potent compared with vehicle sample without $A\beta_{1-42}$ oligomers (Fig. 7a and b). Samples treated with PGG reduced the fluorescence intensity in a concentration-dependent manner (Fig. 7c–e). These data confirmed that PGG was a strong inhibitor of $A\beta_{1-42}$ oligomerization.

Neuroprotective effects of PGG against Aβ toxicity

To evaluate whether PGG could potentially prevent Aβ-induced toxicity, we pre-incubated SK-N-SH cells for 30 min with PGG, followed by 24 h treatment with 10 μM aggregated $A\beta_{1-42}$. SK-N-SH cell viability was significantly impaired by Aβ peptides, measured by MTT assay. PGG (10 μM) significantly protected SK-N-SH cells against Aβ-induced toxicity. When measured by MTT reduction, cell survival was restored from 56.9 ± 2.5% to 87.0 ± 13.6% in response to the $A\beta_{1-42}$ aggregates (Fig. 8).

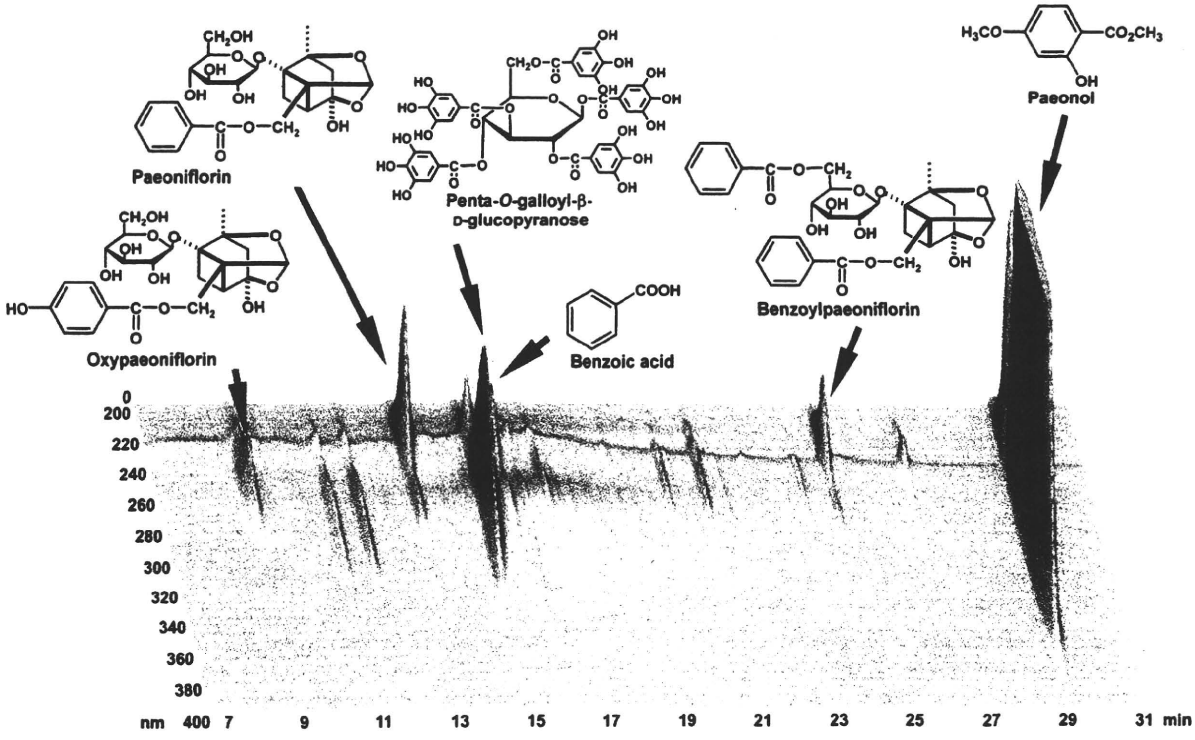

Fig. 4 Identification of chemicals by three-dimensional HPLC analysis of the water extract of *Paeonia suffruticosa*. Each peak indicates a molecule described in the figure.

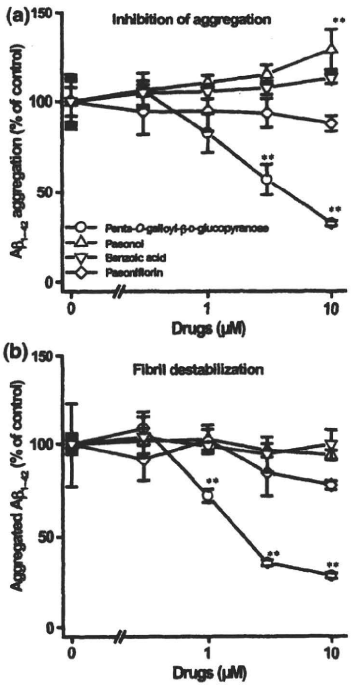

Fig. 5 Effects of distinct compounds isolated from *Paeonia suffruticosa* on the kinetics of Aβs formation and destabilization. a: Aβ aggregate-formation assay. Reaction mixtures containing 20 μM of $A\beta_{1-42}$, 50 mM phosphate buffer (pH 7.4), and various compounds [1,2,3,4,6-penta-*O*-galloyl-β-D-glucopyranose (circles), paeonol (upward-pointing triangles), benzoic acid (downward-pointing triangles), and paeoniflorin (diamond)] were incubated at 37°C for 24 h. Aβ aggregation is expressed as percentage of control observed in the absence of test compounds. b: Aβ aggregate-destabilization assay. Reaction mixtures containing 20 μM $A\beta_{1-42}$ were incubated at 37°C for 24 h. The extracts were added and incubated for 30 min. Aβ aggregation was assessed by the thioflavin T method and expressed as percentage of control aggregation observed in the absence of test compounds. Values represent mean ± SD from four independent experiments. $^{**}p < 0.01$ compared with extract-untreated control.

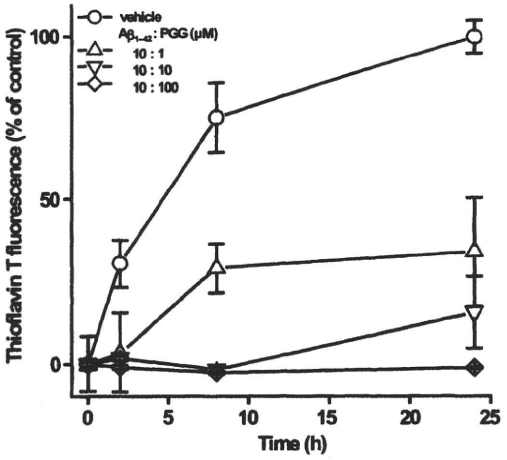

Fig. 6 The molar ratio of the Aβ–PGG interaction. Reaction mixtures containing 10 μM $A\beta_{1-42}$: PGG [solvent alone (circles), molar ratio 10 : 1 (upward-pointing triangles), 10 : 10 (downward-pointing triangles), and 10 : 100 (diamond)] were incubated at 37°C for indicated time. Thioflavin T fluorescence was expressed as a percentage of control which was observed at the point of 24 h without PGG. Values represent mean ± SD from four independent experiments.

Aβ pathology is diminished in PGG-treated Tg mice

To determine the effect of oral PGG treatment accumulation of Aβ in Tg type mice, we evaluated Aβ immunoreactivity in brain sections from untreated and PGG-treated mice by using antibodies BA27 and BC05 (Fig. 9a–d). The number of Aβ-positive spots in the hippocampus was obviously lower in PGG-treated mice (Fig. 9b and d) compared with untreated mice (Fig. 9a and c). No Aβ immunoreactivity was observed in brain sections from non-transgenic mice (data not shown).

We next measured the levels of $A\beta_{1-40}$ and $A\beta_{1-42}$ in brain samples from Tg mice by using a sensitive ELISA method (Fig. 9e and f). In the brains of Tg mice treated with PGG by repeated oral administration, the $A\beta_{1-40}$ and $A\beta_{1-42}$ concentrations were significantly lower (2417.5 ± 279.5% and 46.8 ± 3.0%, $p < 0.01$) than those in PGG-untreated mice. The levels of $A\beta_{1-40}$ and $A\beta_{1-42}$ were below the limit of detection in cerebral cortex samples from non-transgenic mice (data not shown).

Discussion

In AD research, much attention has focused on altering the course of the disease through early diagnosis and intervention. Clinical application of biomarkers and amyloid imaging may be attractive and realistic diagnostic procedures by which to identify the disease early. On the other hand, safety is an important concern with regard to early intervention with disease modifying drugs. *Paeonia suffruticosa* has been used medicinally in humans for more than 1000 years with virtually no toxic effects reported.

The results of our studies using thioflavin T fluorescence demonstrated that *Paeonia suffruticosa* extracts, regardless of the extraction method used, could inhibit the assembly of Aβ fibrils. All three extracts (water, methanol, and ethanol) induced a dramatic decline in the fluorescence intensity of thioflavin T in the μg/mL range. In our preliminary experiment, we confirmed that these extracts did not quench thioflavin T fluorescence at the indicated concentrations. These results suggest two possibilities; one is that *Paeonia suffruticosa* indeed destabilizes Aβ fibrils, and the other is that it antagonizes the binding of thioflavin T to Aβ. It has been reported that absorbance of Congo red was increased by binding to Aβ protein as well as to thioflavin T. The binding site in Aβ to Congo red was different from that to thioflavin

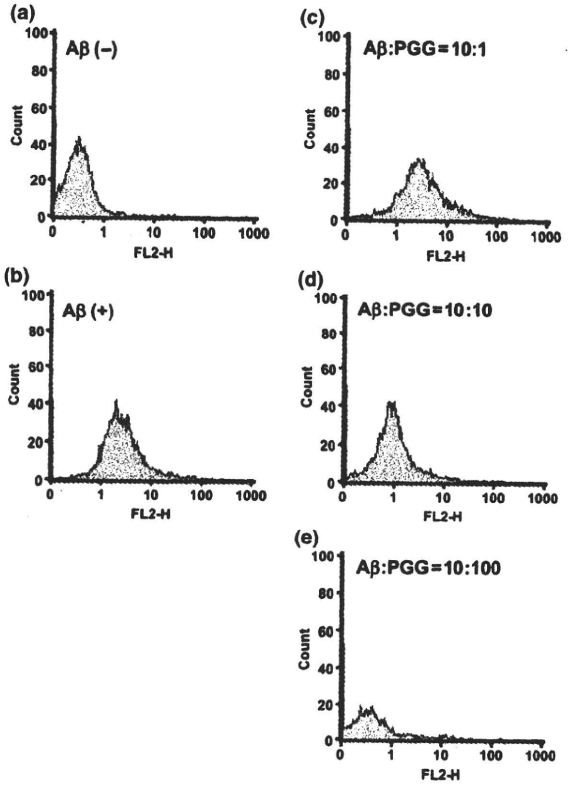

Fig. 7 Effects of PGG on $A\beta_{1-42}$ oligomeric species. These histograms were developed using reagents provided in the Aggregated Aβ Assay Kit. a: buffer-control; b: 10 μM $A\beta_{1-42}$ in absent of PGG; c–e: 10 μM $A\beta_{1-42}$ with PGG molar ratio 10 : 1 (c), 10 : 10 (d), and 10 : 100 (e).

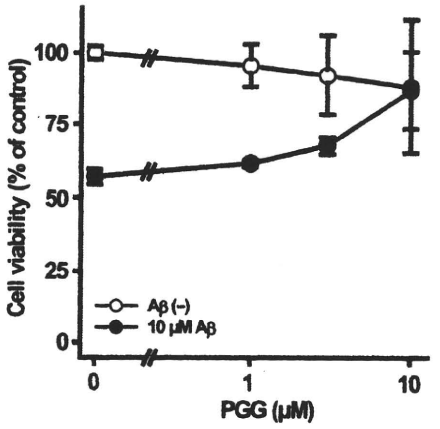

Fig. 8 Effects of PGG against Aβ-induced toxicity. SK-N-SH cells were pre-treated without or with PGG for 30 min followed by incubation without or with $A\beta_{1-42}$ (10 μM) for 24 h. Cell viability was assessed by MTT method and expressed as a percentage of control viability, which was observed in the absence of $A\beta_{1-42}$ and PGG. Values represent the means ± SD from four independent experiments.

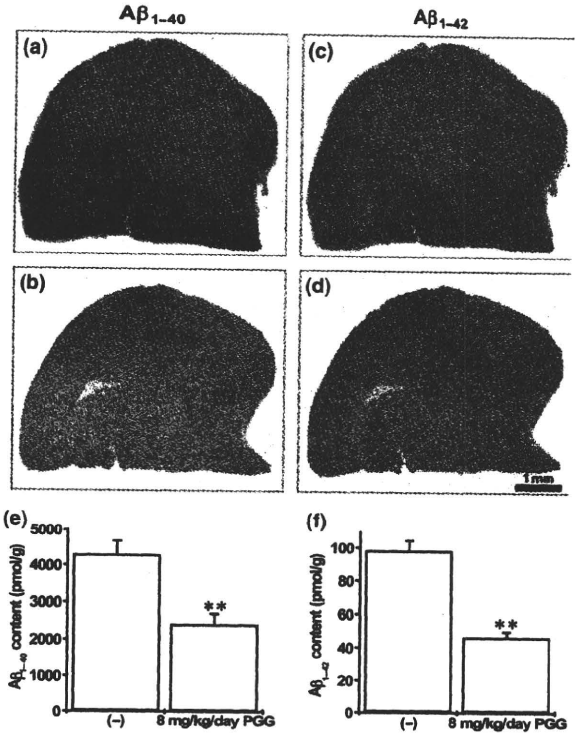

Fig. 9 Immunostaining (a–d) and ELISA analysis of formic acid-extractable Aβ levels (e and f) after dietary intake of 1,2,3,4,6-penta-*O*-galloyl-β-D-glucopyranose (PGG) in Tg2576 mice. (a–d) Hemibrain cryostat sections were labeled with anti- $A\beta_{1-40}$ (a and b) and $A\beta_{1-42}$ (c and d) antibody. Image analysis was performed on the cerebral cortices from PGG-untreated (a and c) and -treated (b and d) animals. Scale bar = 1 mm. Levels of $A\beta_{1-40}$ (e) and $A\beta_{1-42}$ (f) were quantified on formic acid-extractable Aβ from cortices of the 8 mg/kg/day PGG groups. Values represent mean ± SD from seven to eight independent experiments. $^{**}p < 0.01$, compared with PGG-untreated control.

T. In our experiments, each of the three *Paeonia suffruticosa* extracts decreased the absorbance of Congo red (data not shown), suggesting that the decrease in thioflavin T fluorescence by *Paeonia suffruticosa* extracts was caused by destabilization of Aβ fibrils. Moreover, our preliminary atomic force microscopy data also strongly support this notion, as destabilization of Aβ fibrils by *Paeonia suffruticosa* extracts was directly visualized (data not shown). The extracts of *Paeonia suffruticosa* inhibited aggregation of both $A\beta_{1-40}$ and $A\beta_{1-42}$ to a similar extent. Therefore, the inhibitory effect of *Paeonia suffruticosa* on amyloidogenesis of Aβ may not be dependent on the distinct amino acid sequence of its C-terminal.

Paeonia suffruticosa treatment prevented Aβ-related memory deficits and AD-type neuropathology *in vivo*. In our study, we found that treatment of Tg2576 mice with *Paeonia suffruticosa* attenuated memory deterioration, and this effect coincided with an approximately 20% reduction in

Aβ peptide content in the brain. We hypothesize that treatment with *Paeonia suffruticosa* may have beneficial effects on AD-type memory deterioration through a direct interaction between *Paeonia suffruticosa* and Aβ peptides in the brain, leading to the prevention of Aβ plaque formation.

Our studies also showed that PGG at low concentrations (IC_{50} = 3 μM) can inhibit Aβ aggregation or promote its destabilization. Moreover, our preliminary scanning electron microscopy data also strongly support this notion, as destabilization of Aβ fibrils by PGG was directly visualized (Fig. S1). As other chemical compounds, such as paeonol, benzoic acid, and paeoniflorin had no effects on Aβ aggregation, PGG may be the principal active constituent responsible for the effect of *Paeonia suffruticosa* on Aβ fibril regulation. Previous published literatures reported that several polyphenols, such as those from green tea or grape, had anti-aggregation property (Ehrnhoefer *et al.* 2008; Rivière *et al.* 2008). PGG had a comparable inhibitory effect with such published polyphenols.

The toxicity of Aβ is becoming more strongly linked to the formation of oligomeric aggregates (Kirkitadze *et al.* 2002). In our experiments, PGG inhibited Aβ oligomerization. Moreover, treatment of SK-N-SH cells with PGG significantly protected the cells from $Aβ_{1-42}$ toxicity at concentrations similar to those that inhibited Aβ aggregation. Thus, our experiments suggest that PGG inhibited not only Aβ fibril formation but also neurotoxic Aβ oligomer formation. Furthermore, oral intake of PGG reduced Aβ plaque burden and Aβ peptide content in brain tissue from Tg2576 mice, as did like *Paeonia suffruticosa*. There are two possible explanations; one is that PGG indeed destabilizes Aβ fibrils, and the other is that it inhibits the Aβ production or its secretion in Tg2576 mice brain. We demonstrated that PGG did not affect the level of full-length APP in Tg2576 mice (Figure S2), suggesting that the decrease in Aβ plaques and Aβ peptide content in brain tissue from Tg2576 mice by PGG may be caused by destabilization of Aβ fibrils. Curcumin, an active compound of *Curcuma longa*, was reported to inhibit Aβ fibril formation and to destabilize preformed Aβ fibrils *in vitro* and *in vivo* (Ono *et al.* 2004; Yang *et al.* 2005). It has also been reported that this compound is highly hydrophobic and should readily enter the brain to bind to plaques *in vivo* (Yang *et al.* 2005). Although highly hydrophilic, unlike curcumin, PGG has curcumin-like activity on Aβ fibril regulation *in vivo*. Studies of the metabolism of PGG and its ability to penetrate the blood-brain barrier by this compound are now underway.

In conclusion, our study demonstrates that *Paeonia suffruticosa* and PGG not only inhibit Aβ fibril formation but also disassemble pre-formed Aβ fibrils. Moreover, our experiments suggest that PGG inhibits Aβ oligomerization and Aβ toxicity. As a result, it improved memory deficits in Tg2576 mice. Therefore, extracts of *Paeonia suffruticosa* and PGG could have potential as therapeutic drugs for AD patients and may also be useful as primary or secondary preventive agents for healthy individuals and patients with mild cognitive impairment. Furthermore, *Paeonia suffruticosa* has a satisfactory safety profile because no obvious adverse effects of *Pilulae octo-medicamentorum rehmanniae* have been reported. In our preliminary experiments, *Paeonia suffruticosa* was tested for hepatotoxicity, nephrotoxicity, and other biochemical parameters in transgenic mice. Fortunately, this medicinal herb did not show any signs of organ toxicity. Thus, *Paeonia suffruticosa* appears to be a safe natural product for regulating Aβ aggregation. *Paeonia suffruticosa* and PGG may represent a new class of therapeutic and preventive agents for AD which act to regulate the formation and the clearance of senile plaques.

Acknowledgements

This work was partially supported by (i) a grant-in-aid for scientific research from the Ministry of Education, Science, Sports and Culture of Japan (#16590554), (ii) a program for the promotion of fundamental studies in Health Science of the National Institute of Biomedical Innovation (NIBIO) of Japan (#03-1), and (iii) a grant-in-aid from Core Research for Evolutional Science and Technology of Japan Science and Technology Corporation. We thank S. Isogami and M. Takahashi for kind advice and technical supports.

Supporting Information

Additional Supporting Information may be found in the online version of this article:

Figure S1 Scanning electron microscope imaging of $Aβ_{1-42}$ fibrils. After incubation of $Aβ_{1-42}$ for 24 h for preformed fibrils, the mixture of aggregated Aβ and the PGG was incubated at 37°C for 1 h. A: vehicle (DMSO); B: 10 μM $Aβ_{1-42}$: 10 μM PGG (molar ratio 1 : 1). Scale bar = 5 μm.

Figure S2 Effects of PGG on the level of amyloid precursor protein (APP) in Tg2576 mice. Immunoblotting of brain levels of APP after dietary 1,2,3,4,6-penta-*O*-galloyl-β-D-glucopyranose (PGG) in Tg2576. Levels of APP were quantitated by immunoblotting with full length APP antibody from cortices of 8 mg/kg/day-PGG groups. The samples were separated on a 10% polyacrylamide gel, followed by immunoblotting with anti-full length APP antibody. Arrowheads point to APP. Similar results were obtained from at least 3 independent experiments.

Please note: Wiley-Blackwell are not responsible for the content or functionality of any supporting materials supplied by the authors. Any queries (other than missing material) should be directed to the corresponding author for the article.

References

Anderton B. H., Callahan L., Coleman P. *et al.* (1998) Dendritic changes in Alzheimer's disease and factors that may underlie these changes. *Prog. Neurobiol.* **55**, 595–609.

Barghorn S., Nimmrich V., Striebinger A. *et al.* (2005) Globular amyloid beta-peptide oligomer – a homogenous and stable neuropathological protein in Alzheimer's disease. *J. Neurochem.* **95**, 834–847.

Barrow C. J. and Zagorski M. G. (1991) Solution Structures of β-peptide and its constituent fragments: relation to amyloid deposition. *Science* **253**, 179–182.

Calon F., Lim G. P., Yang F. *et al.* (2004) Docosahexaenoic acid protects from dendritic pathology in an Alzheimer's disease mouse model. *Neuron* **43**, 633–645.

Chou T. C. (2003) Anti-inflammatory and analgesic effects of Paeonol in carrageenan-evoked thermal hyperalgesia. *Br. J. Pharmacol.* **139**, 1146–1152.

Darreh-Shori T., Hellstrom-Lindahl E., Flores-Flores C. *et al.* (2004) Long-lasting acetylcholinesterase splice variations in anticholinesterase-treated Alzheimer's disease patients. *J. Neurochem.* **88**, 1102–1113.

Ehrnhoefer D. E., Bieschke J., Boeddrich A. *et al.* (2008) EGCG redirects amyloidogenic polypeptides into unstructured, off-pathway oligomers. *Nat. Struct. Mol. Biol.* **15**, 558–566.

Fujiwara H., Iwasaki K., Furukawa K. *et al.* (2006) *Uncaria rhynchophylla*, a Chinese medicinal herb, has potent antiaggregation effects on Alzheimer's beta-amyloid proteins. *J. Neurosci. Res.* **84**, 427–433.

Hofmann T., Glabasnia A., Schwarz B. *et al.* (2006) Protein binding and astringent taste of a polymeric procyanidin, 1,2,3,4,6-penta-*O*-galloyl-beta-D-glucopyranose, castalagin, and grandinin. *J. Agric. Food. Chem.* **54**, 9503–9509.

Hsieh C. L., Cheng C. Y. and Tsai T. H. (2006) Paeonol reduced cerebral infarction involving the superoxide anion and microglia activation in ischemia-reperfusion injured rats. *J. Ethnopharmacol.* **106**, 208–215.

Iwasaki K., Kobayashi S., Chimura Y. *et al.* (2004) A randomized, double-blind, placebo-controlled clinical trial of the Chinese medicinal herb "ba wei di huang wan" in the treatment of dementia. *J. Am. Geriatr. Soc.* **52**, 1518–1521.

Iwasaki K., Satoh-Nakagawa T., Maruyama M. *et al.* (2005) A randomized, observer-blind, controlled trial of the traditional Chinese medicine Yi-Gan San for improvement of behavioral and psychological symptoms and activities of daily living in dementia patients. *J. Clin. Psychiatry* **66**, 248–252.

Kirkitadze M. D., Bitan G. and Teplow D. B. (2002) Paradigm shifts in Alzheimer's disease and other neurodegenerative disorders: the emerging role of oligomeric assemblies. *J. Neurosci. Res.* **69**, 567–577.

Le Bars P. L., Katz M. M., Berman N. *et al.* (1997) A placebo-controlled, double-blind, randomized trial of an extract of Ginkgo biloba for dementia. North American EGb Study Group. *JAMA* **278**, 1327–1332.

Li Y., Kim J., Li J. *et al.* (2005) Natural anti-diabetic compound 1,2,3,4,6-penta-*O*-galloyl-D-glucopyranose binds to insulin receptor and activates insulin-mediated glucose transport signaling pathway. *Biochem. Biophys. Res. Commun.* **336**, 430–437.

Lin H. C., Ding H. Y., Ko F. N. *et al.* (1999) Aggregation inhibitory activity of minor acetophenones from *Paeonia* species. *Planta Med.* **65**, 595–599.

Millard C. B. and Broomfield C. A. (1995) Anticholinesterases: medical applications of neurochemical principles. *J. Neurochem.* **64**, 1909–1918.

Nakagawasai O., Yamadera F., Iwasaki K. *et al.* (2004) Effect of kami-untan-to on the impairment of learning and memory induced by thiamine-deficient feeding in mice. *Neuroscience* **125**, 233–241.

Ono K., Hasegawa K., Naiki H. *et al.* (2004) Curcumin has potent anti-amyloidogenic effects for Alzheimer's beta-amyloid fibrils in vitro. *J. Neurosci. Res.* **75**, 742–750.

Park C. H., Lee Y. J., Lee S. H. *et al.* (2000) Dehydroevodiamine HCl prevents impairment of learning and memory and neuronal loss in rat models of cognitive disturbance. *J. Neurochem.* **74**, 244–253.

Rivière C., Richard T., Vitrac X. *et al.* (2008) New polyphenols active on beta-amyloid aggregation. *Bioorg. Med. Chem. Lett.* **18**, 828–831.

Selkoe D. J. (2002) Alzheimer's disease is a synaptic failure. *Science* **298**, 789–791.

Suemoto T., Okamura N., Shiomitsu T. *et al.* (2004) *In vivo* labeling of amyloid with BF-108. *Neurosci. Res.* **48**, 65–74.

Suzuki T., Arai H., Iwasaki K. *et al.* (2001) A Japanese herbal medicine (Kami-Untan-To) in the treatment of Alzheimer's disease: A pilot study. *Alzheimer's Rep.* **4**, 177–182.

Tierney M. C., Fisher R. H., Lewis A. J. *et al.* (1988) The NINCDS-ADRDA Work Group criteria for the clinical diagnosis of probable Alzheimer's disease: a clinicopathologic study of 57 cases. *Neurology* **38**, 346–359.

Wirths O., Multhaup G. and Bayer T. A. (2004) A modified β-amyloid hypothesis: intraneuronal accumulation of the β-amyloid peptide – the first step of a fatal cascade. *J. Neurochem.* **91**, 513–520.

Yang F., Lim G. P., Begum A. N. *et al.* (2005) Curcumin inhibits formation of amyloid beta oligomers and fibrils, binds plaques, and reduces amyloid in vivo. *J. Biol. Chem.* **280**, 5892–5901.

Yasuda T., Kon R., Nakazawa T. *et al.* (1999) Metabolism of Paeonol in rats. *J. Nat. Prod.* **62**, 1142–1144.

THE JOURNAL OF BIOLOGICAL CHEMISTRY VOL. 284, NO. 48, pp. 33400–33408, November 27, 2009

Depletion of Vitamin E Increases Amyloid β Accumulation by Decreasing Its Clearances from Brain and Blood in a Mouse Model of Alzheimer Disease*[S]

Received for publication, August 9, 2009 Published, JBC Papers in Press, August 13, 2009, DOI 10.1074/jbc.M109.054056

Yoichiro Nishida[‡], Shingo Ito[§], Sumio Ohtsuki[§], Naoki Yamamoto[¶], Tsubura Takahashi[‡], Nobuhisa Iwata[‖], Kou-ichi Jishage[**], Hiromi Yamada[‡], Hiroki Sasaguri[‡], Shigefumi Yokota[‡], Wenying Piao[‡], Hiroyuki Tomimitsu[‡], Takaomi C. Saido[‖], Katsuhiko Yanagisawa[¶], Tetsuya Terasaki[§], Hidehiro Mizusawa[‡], and Takanori Yokota[‡1]

From the [‡]Department of Neurology and Neurological Science, Graduate School, Tokyo Medical and Dental University, 1-5-45 Yushima, Bunkyo-ku, Tokyo 113-8519, the [§]Department of Molecular Biopharmacy and Genetics, Graduate School of Pharmaceutical Sciences, Tohoku University, Aoba, Aramaki, Aoba-ku, Sendai, Miyagi 980-8578, the [¶]National Institute for Longevity Sciences, National Center for Geriatrics and Gerontology, 36-3 Gengo, Morioka, Obu, Aichi 474-8522, the [‖]Laboratory for Proteolytic Neuroscience, RIKEN Brain Science Institute, 2-1 Hirosawa, Wako-shi, Saitama 351-0198, and the [**]Chugai Research Institute for Medical Science, Inc., Gotenba, Shizuoka 412-8513, Japan

Increased oxidative damage is a prominent and early feature in Alzheimer disease. We previously crossed Alzheimer disease transgenic (*APPsw*) model mice with α-tocopherol transfer protein knock-out (*Ttpa*$^{-/-}$) mice in which lipid peroxidation in the brain was significantly increased. The resulting double-mutant (*Ttpa*$^{-/-}$*APPsw*) mice showed increased amyloid β (Aβ) deposits in the brain, which was ameliorated with α-tocopherol supplementation. To investigate the mechanism of the increased Aβ accumulation, we here studied generation, degradation, aggregation, and efflux of Aβ in the mice. The clearance of intracerebral-microinjected ^{125}I-Aβ$_{1-40}$ from brain was decreased in *Ttpa*$^{-/-}$ mice to be compared with wild-type mice, whereas the generation of Aβ was not increased in *Ttpa*$^{-/-}$*APPsw* mice. The activity of an Aβ-degrading enzyme, neprilysin, did not decrease, but the expression level of insulin-degrading enzyme was markedly decreased in *Ttpa*$^{-/-}$ mouse brain. In contrast, Aβ aggregation was accelerated in *Ttpa*$^{-/-}$ mouse brains compared with wild-type brains, and well known molecules involved in Aβ transport from brain to blood, low density lipoprotein receptor-related protein-1 (LRP-1) and p-glycoprotein, were up-regulated in the small vascular fraction of *Ttpa*$^{-/-}$ mouse brains. Moreover, the disappearance of intravenously administered ^{125}I-Aβ$_{1-40}$ was decreased in *Ttpa*$^{-/-}$ mice with reduced translocation of LRP-1 in the hepatocytes. These results suggest that lipid peroxidation due to depletion of α-tocopherol impairs Aβ clearances from the brain and from the blood, possibly causing increased Aβ accumulation in *Ttpa*$^{-/-}$*APPsw* mouse brain and plasma.

The accumulation of amyloid β (Aβ)[2] is the primary pathological event driving neurodegeneration in Alzheimer disease (AD). Support of this hypothesis is based on genetic evidence from cases of familial AD with β-amyloid precursor protein (APP) or presenilin mutations and the remarkable effect of Aβ elimination by its vaccine on AD phenotype. The suggested mechanism for Aβ accumulation in sporadic AD includes elevated generation of Aβ due to increased β-secretase activity (1), decreased degradation of Aβ (2), and decreased efflux of Aβ from the brain to blood (3).

Increased oxidative stress of brain is a key feature of sporadic AD and manifests predominantly as lipid peroxidation (4). There are several lines of evidence suggesting that the AD brain displays extensive oxidative damage to various biological macromolecules, including lipids, proteins, and nucleic acids (5). Both Aβ level and lipid peroxidation in the brain are increased with disease progression of AD. However, the direct relationship between Aβ accumulation and lipid peroxidation is unclear (6).

Among natural isomers of vitamin E, α-tocopherol (α-Toc) has the most potent biological activity and is a major antioxidant that protects polyunsaturated fatty acids from peroxidation. Brain α-Toc content is maintained by α-tocopherol transfer protein (α-TTP), which transfers α-Toc from chylomicron to very low-density lipoprotein in the liver and transports α-Toc from blood to brain (7, 8). We have developed an α-tocopherol transfer protein knock-out (*Ttpa*$^{-/-}$) mouse that showed marked lipid peroxidation because of a lack of α-Toc in the brain and considered it as a model for chronic oxidative stress to the brain (7). In a *Ttpa*$^{-/-}$ mouse brain, two lipid peroxidation markers, thiobarbituric acid reactive substrates

* This work was supported in part by a grant for Research on Psychiatric and Neurological Disease and Mental Health from the Ministry of Health, Labor, and Welfare of Japan (to T. Y. and H. M.), a grant from the 21st Century COE Program on Brain Integration and Its Disorders to Tokyo Medical and Dental University (to Y. N., H. S., and H. M.), a grant from the Ministry of Education, Science, and Culture (to N. I., H. T., T. Y., and H. T.), and a grant of the SORST of Japan Science and Technology Agency (to S. O. and T. Terasaki).

[S] The on-line version of this article (available at http://www.jbc.org) contains supplemental Tables 1–3.

[1] To whom correspondence should be addressed. Tel.: 81-3-5803-5234; Fax: 81-3-5803-0169; E-mail: tak-yokota.nuro@tmd.ac.jp.

[2] The abbreviations used are: Aβ, amyloid β; AD, Alzheimer disease; APP, β-amyloid precursor protein; α-TTP, α-tocopherol transfer protein; PBS, phosphate-buffered saline; BBB, blood-brain barrier; LRP-1, lipoprotein receptor-related protein-1; Pgp, p-glycoprotein; GLUT-1, glucose transporter-1; TTR, transthyretin; BEI, brain efflux index; CLtot, total body clearance; α-Toc, α-tocopherol; TBS, Tris-buffered saline; PIPES, 1,4-piperazinediethanesulfonic acid; CHAPS, 3-[(3-cholamidopropyl)dimethylammonio]-1-propanesulfonic acid; IDE, insulin-degrading enzyme.

and 4-hydroxynonenal, were increased, and lipofuscin was massively accumulated (7). It is of note that the same markers were elevated in AD brains (9–11). We previously crossed the AD transgenic (*APPsw*) model mouse (Tg2576) with *Ttpa*$^{-/-}$ mouse, and the resulting double-mutant (*Ttpa*$^{-/-}$*APPsw*) mouse showed earlier and more severe cognitive dysfunction and had increased amyloid plaques in the brain by depletion of α-Toc (12). As a next step, we have studied the mechanism of how chronic lipid peroxidation increased Aβ deposits. The studies of the lifecycle of Aβ from its generation to its metabolism have received an extraordinary amount of attention in the field of AD research. Although the Aβ level in the brain is determined by the rate of Aβ generation and clearance in the brain, the clearance of Aβ from circulation is also important for the Aβ accumulation in the brain, because the Aβ levels in the brain and in the blood are held in equilibrium (3). Therefore, we evaluated the Aβ generation in the brain and its clearance from the brain and from the blood in *Ttpa*$^{-/-}$ mouse. We also measured the aggregation capacity of Aβ in the brain to evaluate the effect of oxidative stress on the accumulation of Aβ in the brain.

EXPERIMENTAL PROCEDURES

Animals

All experiments were approved by the Animal Experiment Committees of Tokyo Medical and Dental University. We used *Ttpa*$^{-/-}$ mice from a C57BL/6J background (7). We crossbred *Ttpa*$^{-/-}$ mice with *APPsw* transgene hemizygous mice (Tg2576 from a C57BL/6-SJL background, Taconic, Hudson, NY), which is an AD model that overexpresses a human APP_{695} with a double mutation (*APPsw*; K670N,M671L) (13). We then cross-bred *Ttpa*$^{+/-}$*APPsw* and *Ttpa*$^{+/-}$ to produce the *Ttpa*$^{-/-}$*APPsw* mice. Animals were screened for the presence of APPsw and α-TTP genes by PCR analysis of tail DNA. Complete elimination of α-Toc from the brain is achieved only when the deletion of α-TTP gene is combined with the dietary restriction, because a part of α-Toc taken up from the small intestine can enter the brain even without α-TTP (7). Furthermore, it is impossible to produce mice with α-Toc-deficient diet because supplementation of α-Toc is necessary for the maintenance of pregnancy (7). The dietary restriction of α-Toc after birth could not eliminate α-Toc from the brain of wild-type mice (7). Therefore, to study the effect of α-Toc depletion on AD phenotype, we fed the resulting double mutant (*Ttpa*$^{-/-}$*APPsw*) mice on α-Toc-deficient diet (Funabashi Farm, Chiba, Japan) and compared with the *APPsw* littermate mice on normal diet (36 mg of α-Toc/kg). To determine whether the differences in the phenotypes between *APPsw* mice and *Ttpa*$^{-/-}$*APPsw* mice are caused by the *Ttpa*$^{-/-}$ gene effect or α-Toc-deficient effect, we furthermore made a group of *Ttpa*$^{-/-}$*APPsw* mice that were fed on α-Toc-supplemented diet (750 mg of α-Toc/kg, Funabashi Farm). Details for these diets were previously described (7). All mice were housed in plastic cages, received food and water *ad libitum*, and were maintained on a 12/12-h light-dark cycle (lights on at 09:00, off at 21:00).

Aβ Quantitation in the Brain and Plasma

Three or four 18-month-old mice for each group were anesthetized with an intraperitoneal injection of pentobarbital (60 mg/kg). After blood was collected, they killed by transcardiac perfusion with 0.01 M phosphate-buffered saline (PBS), pH 7.4. The cerebral hemisphere was homogenized in 50 mM Tris-HCl buffer (TBS), pH 7.6, containing 150 mM NaCl and a protease inhibitor mixture (Complete, Roche Diagnostics) supplemented with 0.7 μg/ml pepstatin A (Peptide Institute, Osaka, Japan) with a Teflon glass homogenizer and centrifuged at 200,000 × *g* for 20 min at 4 °C. The supernatant was defined as the TBS-soluble fraction. The pellet was solubilized by sonication in 6 M guanidine-HCl buffer containing a protease inhibitor mixture. The solubilized pellet was centrifuged as before, after which the supernatant was diluted 12-fold to reduce the concentration of guanidine-HCl and used as the TBS-insoluble fraction (guanidine-extractable). The amounts of $Aβ_{1-40}$ and $Aβ_{1-42}$ in each fraction and plasma were assayed using commercially available human $Aβ_{1-40}$ and $Aβ_{1-42}$ sandwich enzyme-linked immunosorbent assay kits (BioSource International, Inc., Camarillo, CA).

Northern Blot Analysis

Three or four 18-month-old mice in each group were examined. Total RNA was extracted from the brain by TRIzol (Invitrogen). Total RNA (2.5 μg) was fractionated in a formaldehyde-agarose gel and transferred to a Nytran membrane (Schleicher & Schuell). The upper part of the membrane was hybridized with a purified PCR fragment corresponding to human APPsw cDNA (bases 981–1578). The lower part was hybridized with a probe specific for glyceraldehyde-3-phosphate dehydrogenase to confirm the quantity of loaded RNA. The signals were visualized with a Gene Images CDP-star detection kit (Amersham Biosciences).

Western Blot Analysis

C-terminal Fragments of APP-β, -α, and -γ/ε—Three or four 18-month-old mice in each group were examined. To analyze C-terminal fragments -β, -α, and -γ/ε, the cerebral hemisphere was homogenized with 50 mM TBS and centrifuged at 800 × *g* for 10 min at 4 °C. The supernatant was centrifuged at 200,000 × *g* for 28 min at 4 °C, and the resultant pellet was resuspended with 20 mM PIPES, pH 7.0, containing 140 mM KCl, 0.25 M sucrose, 5 mM EGTA, and a protease inhibitor mixture. Protein concentration was determined using a BCA protein assay kit (Pierce) and adjusted. After incubation of the suspension at 37 °C for 60 min, it was delipidized with chloroform:methanol (2:1) and chloroform:methanol:distilled water (1:2:0.8) sequentially to improve sensitivity. The resultant protein fraction was dried by evaporation and then solubilized with a sample buffer containing 9 M urea. Samples (20 μg) were separated by 16.5% SDS-polyacrylamide gel electrophoresis and transferred electrophoretically to nitrocellulose membranes (Schleicher & Schuell). The membranes were boiled in PBS for 3 min to improve sensitivity. The blot was probed with the rabbit polyclonal antibody against the C terminus of APP (A8717, Sigma) followed by the avidin-biotin-peroxidase complex (ABC) method (Vectastain ABC kits, Vector Laboratories,

Burlingame, CA). The immunoreactive band on the membrane was visualized with a Supersignal West Pico Chemiluminescence kit (Pierce).

Proteins to Transport Aβ across the Blood-Brain Barrier (BBB)—Three sets of three 8-month-old mice in each group were examined. The vascular fraction of small vessels was prepared from whole cerebrum using a modified method reported previously (14). Briefly, brains were homogenized in 10 mM PBS. After centrifugation at 800 × *g* for 5 min at 4 °C, the pellets were suspended with a dextran solution (M_r 70,000; 15% w/v, Sigma) and centrifuged at 4500 × *g* for 10 min at 4 °C. The pellets were washed by 10 mM PBS twice and resuspended with 5 mM PBS for 10 min. After centrifuging at 800 × *g* for 5 min, the final pellets of small vessels were resuspended by pipetting and vortexed in the homogenization buffer containing 10 mM TBS, pH 7.4, containing 1 mM EDTA, 150 mM NaCl, 4% CHAPS, 1 mM phenylmethylsulfonyl fluoride, and a protease-inhibitor mixture (Complete-Mini, Roche Diagnostics). The 4.5-μg samples were separated by 7.5 and 15% SDS-polyacrylamide mini-gel and transferred to a nitrocellulose membrane. The membrane was probed with mouse anti-low density lipoprotein receptor-related protein-1 (LRP-1) (β-chain specific, American Diagnostica Inc., Stamford, CT) or mouse anti-p-glycoprotein (Pgp) (C219, Signet, Dedham, MA) followed by sheep anti-mouse secondary antibody conjugated to horseradish peroxidase (Amersham Biosciences). Rabbit anti-brain-type glucose transporter-1 (GLUT-1) antibody (Alpha Diagnostic International, San Antonio, TX) with donkey anti-rabbit secondary antibody (Amersham Biosciences) was also used. Bands were visualized by using an ECL Plus Western blotting system (Amersham Biosciences).

Protein to Transport Aβ into the Liver—Three 8-month-old mice in each group were examined. To prepare the crude membrane fraction, liver was homogenized in hypotonic lysis buffer (10 mM Tris, 10 mM NaCl, 1.5 mM $MgCl_2$, pH 7.4) with 1 mM phenylmethylsulfonyl fluoride and a protease-inhibitor mixture (Complete-Mini). After centrifugation at 8000 × *g* for 10 min at 4 °C, the supernatant was centrifuged at 100,000 × *g* for 60 min at 4 °C. The pellet obtained was regarded as the crude membrane fraction. Furthermore, to prepare the plasma membrane fraction of the liver, this obtained pellet was resuspended in 10 mM HEPES, 250 mM sucrose, pH 7.4, and overlaid on 38% sucrose solution and then centrifuged at 100,000 × *g* for 40 min at 4 °C using a swing rotor (SW40Ti; Beckman, Fullerton, CA). The turbid layer was collected and centrifuged at 100,000 × *g* for 1 h at 4 °C, and the obtained pellet was defined as plasma membrane fraction. The 2.5-μg samples were separated with 7.5% SDS-polyacrylamide mini-gel and transferred electrophoretically to a nitrocellulose membrane. The membrane was probed with mouse anti-LRP-1, rabbit anti-cadherin (ab16505, Abcam, Cambridge, UK), or mouse anti-β-actin (A2228, Sigma) followed by sheep anti-mouse secondary antibody conjugated to horseradish peroxidase or a goat anti-rabbit antibody (Pierce), respectively. Bands were visualized by using an ECL Plus Western blotting system or a Supersignal West Femto Maximum Sensitivity kit (Pierce).

Aβ Ligand Proteins in the Plasma—Three or four 14-month-old mice in each group were examined. The collected plasma was diluted with saline, and the 0.10-μl anti-apolipoprotein E (apoE) or 0.40-μl anti-transthyretin (TTR) samples were separated with 15% SDS-polyacrylamide mini-gel and transferred electrophoretically to a polyvinylidene difluoride membrane (Bio-Rad). The membrane was probed with goat polyclonal anti-apoE (sc-6384, Santa Cruz Biotechnology, Inc., Santa Cruz, CA) or rabbit anti-TTR (Dako, Glostrup, Denmark) followed by donkey anti-goat secondary antibody conjugated to horseradish peroxidase (Santa Cruz Biotechnology) or donkey anti-rabbit antibody (Amersham Biosciences). Bands were visualized by using an ECL Plus Western blotting system.

Aβ Degrading Proteins in the Brain—Three or five 23-month-old mice in each group were examined. The cerebral hemisphere was homogenized in homogenization buffer (0.1 M Tris-HCl, pH 8.0, 0.15 M NaCl, 1 mg/ml leupeptin, and 1 mg/ml pepstatin A) and centrifuged at 500 × *g* for 5 min. Membranes were prepared by precipitation of the postnuclear supernatant at 100,000 × *g* for 60 min. The resulting pellet was subjected to protein extraction using 2% SDS by homogenization and posterior centrifugation at 100,000 × *g* for 60 min at 4 °C. The supernatant was used as a membrane fraction. Protein concentration was determined using a BCA protein assay kit, and the membrane fraction (2.5 μg) was separated by 7.5% SDS-polyacrylamide gel electrophoresis and transferred electrophoretically to polyvinylidene difluoride membrane. The blotted membrane was probed with rabbit polyclonal anti-insulin-degrading enzyme (IDE) (Calbiochem) or mouse anti-flotillin (BD Biosciences) followed by donkey anti-rabbit or sheep anti-mouse secondary antibody conjugated to horseradish peroxidase (Amersham Biosciences). Bands were visualized by using an ECL Plus Western blotting system.

β- and γ-Secretase Activities Measurement

The total activities of β- and γ-secretase present in the cerebrum of four 9-month-old mice were determined using secretase-kits (R&D Systems, Wiesbaden, Germany) (15). Secretase enzymatic activities were proportional to the fluorometric reaction, and the data were corrected by subtraction of background control (reactions in the absence of tissue).

Study of Aβ Efflux from the Brain at the BBB

In vivo brain elimination experiments were performed using intracerebral microinjection as described previously (16, 17). Four 2- or 14-month-old mice in each group were anesthetized intramuscularly with a mixture of ketamine (125 mg/kg) and xylazine (1.22 mg/kg), then mounted on a stereotaxic frame (SRS-6, Narishige, Tokyo, Japan) to hold the heads in position. Using a dental drill, a bore hole was made 3.8 mm lateral to the bregma. Then extracellular fluid buffer (122 mM NaCl, 25 mM $NaHCO_3$, 3 mM KCl, 1.4 mM $CaCl_2$, 1.2 mM $MgSO_4$, 0.4 mM K_2HPO_4, 10 mM D-glucose, and 10 mM HEPES, pH 7.4) containing 0.012 μCi of ^{125}I-Aβ_{1-40} and 0.12 μCi of [^{3}H]dextran was injected over a period of 1 min using a 5.0-μl microsyringe (Hamilton, Reno, NE) fitted with a fine needle at a depth of 2.5 mm from the surface of the scalp, *i.e.* in the secondary somatosensory cortex 2 (S2) region. The needle was left in this configuration for an additional 4 min to prevent reflux of the injected solution along the injection track before being slowly retracted.

At the designated times after microinjection, aliquots of cerebrospinal fluid were collected from the cisterna magna as reported previously (17). The whole brain was subsequently removed, and the left cerebrum, right cerebrum, and cerebellum were isolated and dissolved in 2.0 ml of 2 M NaOH at 60 °C for 1 h. The ^{125}I radioactivity of the samples was measured in a γ-counter (ART300, Aloka, Tokyo, Japan) for 3 min. The samples were then mixed with 14 ml of Hionic-fluor (Packard Instrument Co.), and ^{3}H radioactivity was measured in a liquid scintillation counter (TRI-CARB2050CA, Packard Instrument Co.) for 5 min. No radioactivity associated with this efflux transport process was detected in the contralateral cerebrum, cerebellum, or cerebrospinal fluid (data not shown), suggesting the operation of a selective efflux transport process across the BBB. The brain efflux index (BEI) was defined by the equation BEI % = (test substrate undergoing efflux at the BBB)/(test substrate injected into the brain) × 100, and the percentage of substrate remaining in the ipsilateral cerebrum was determined from 100 − BEI (%) = (amount of test substrate in the brain/amount of reference in the brain)/(amount of test substrate injected/amount of injected as a reference in the brain) × 100. The apparent elimination rate constant (k_e) was determined from the slope given by fitting a semilogarithmic plot of 100 − BEI *versus* time using the nonlinear least-squares regression analysis program MULTI (18).

^{125}I-Aβ$_{1-40}$ Plasma Pharmacokinetic Studies

Four or five 2- and 25-month-old mice in each group were anesthetized intramuscularly with a mixture of ketamine (125 mg/kg) and xylazine (1.22 mg/kg), and the jugular vein was isolated. Their body temperature was kept at 37 °C on a hot plate. Each mouse received a bolus intravenous injection of ^{125}I-Aβ$_{1-40}$ (5 μCi; 100 μl) into the jugular vein. Blood samples (30 μl) were collected from the tail vein by using a heparinized microcapillary at various intervals (1, 3, 5, 10, 15, 30, 60, 120, and 360 min) after the injection. The blood samples were centrifuged at 10,000 × *g* for 5 min at 4 °C, and the supernatant was obtained. To assess the integrity of the peptides, a plasma aliquot at each time point was cold-precipitated with 10% trichloroacetic acid in saline. After trichloroacetic acid precipitation, the precipitant was dissolved in 200 μl of 2 M NaOH at 55 °C for 10 min. The ^{125}I radioactivity of the samples was measured in a γ-counter (ART300) for 3 min.

The plasma concentration *versus* time data were analyzed by MOMENT (19) based on the model-independent moment analysis method (20). Briefly, the area under the plasma concentration-time curve (AUC) extrapolated to infinity was calculated the equation AUC = AUC_{0-360} + C_{360}/k_e, in which AUC_{0-360} is the area under the curve from time 0 to the time of the last plasma sample at 360 min calculated by the log-trapezoidal method, C_{360} is plasma concentration of the last plasma sample at 360 min, and k_e is the terminal elimination rate constant estimated from terminal points using the Akaike's Information Criterion-based method. The total body clearance (CLtot) was calculated by the equation CLtot = dose/AUC, where dose is the administered amount of ^{125}I-Aβ$_{1-40}$. The mean residence time (MRT) and the steady-state volume of distribution (Vdss) were calculated by MRT = AUMC/AUC and Vdss = CL·MRT, where AUMC is the total area under the first-moment time curve extrapolated to infinity.

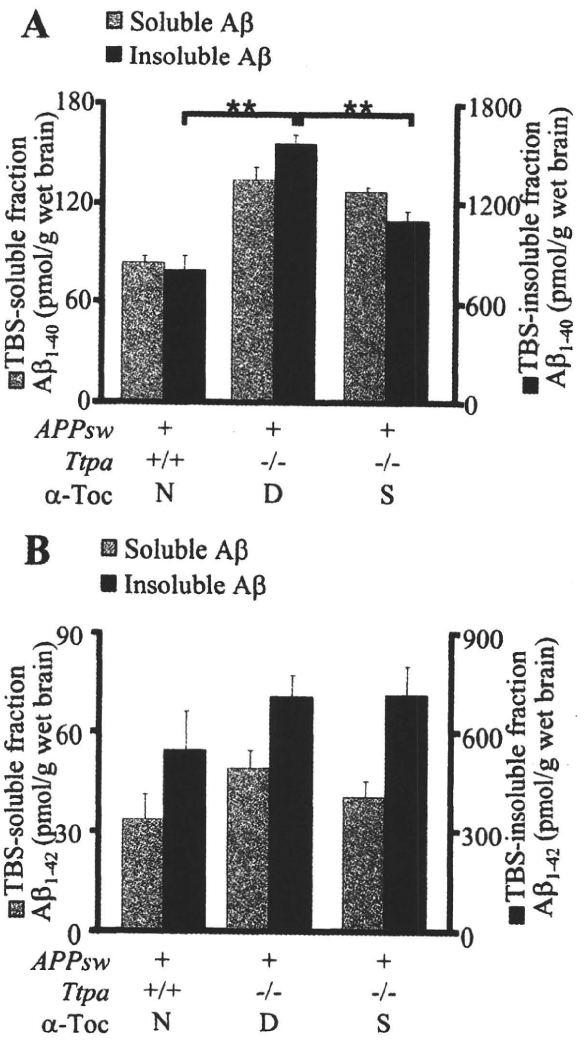

FIGURE 1. **The *Ttpa*$^{-/-}$*APPsw* mouse shows enhanced accumulation of Aβ in the brain.** *A* and *B*, cerebral Aβ$_{1-40}$ (*A*) and Aβ$_{1-42}$ (*B*) levels in 18-month-old mice. *Ttpa*$^{-/-}$*APPsw* mice showed increased level of Aβ$_{1-40}$ in the TBS-insoluble fraction of the brain homogenate and a similar tendency of increase of Aβ$_{1-40}$ and Aβ$_{1-42}$ in other fractions. This increase was partially ameliorated by α-Toc supplementation in the diet. *D*, α-Toc-deficient diet; *S*, α-Toc-supplemented diet; *N*, normal diet. **, $p < 0.01$.

Assay of Neprilysin-dependent Neutral Endopeptidase Activity

Four 4-month-old mice in each group were examined. Triton X-100-solubilized membrane fraction from brain was prepared to assay neutral endopeptidase activity as described previously (21). The neprilysin-dependent neutral endopeptidase activity was fluorometrically assayed using 0.1 mM succinyl-Ala-Ala-Phe-amidomethylcoumarin (Bachem, Bubendorf, Switzerland) as a substrate and determined from the fluorescence intensity (excitation, 390 nm; emission, 460 nm), based on the decrease in the rate of digestion caused by 0.1 μM thiorphan, a specific inhibitor of neprilysin.

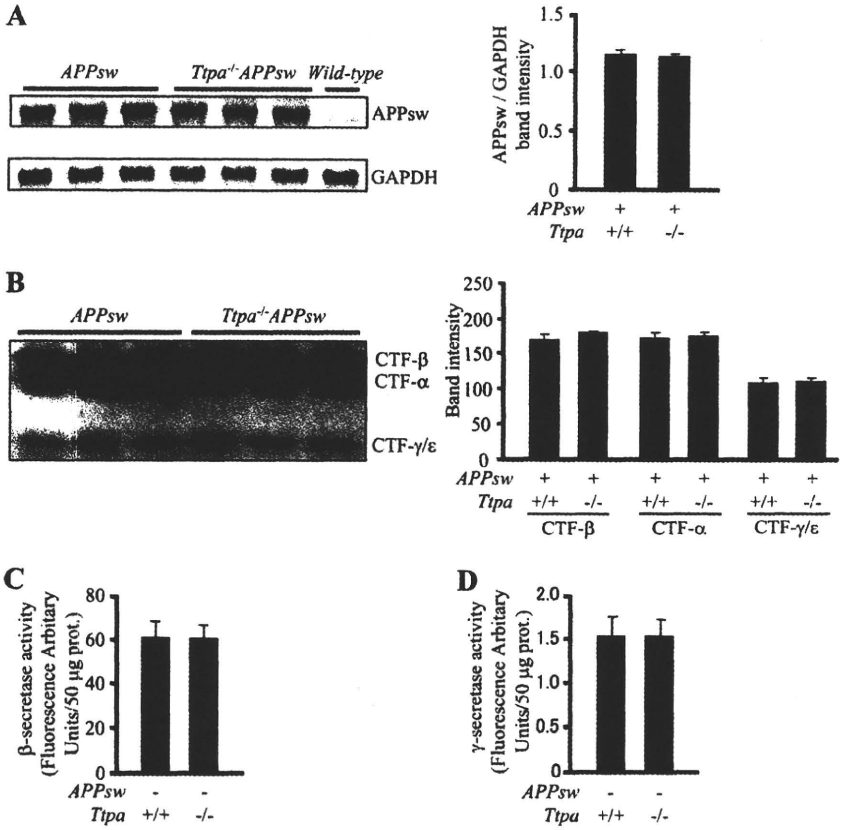

FIGURE 2. **α-Toc depletion does not increase APP expression nor β/γ-cleavages.** *A*, the human APPsw mRNA expression did not increase in the brains of *Ttpa*$^{-/-}$*APPsw* mice compared with *APPsw* mice. The band intensities normalized to the mouse glyceraldehyde-3-phosphate dehydrogenase (*GAPDH*) bands are shown in the *right panel*. *B*, protein levels of C-terminal fragments of APP-β, -α, and -γ/ε did not change in the brains of *Ttpa*$^{-/-}$*APPsw* mice compared with *APPsw* mice. Band intensities are shown in the *right panel*. *C* and *D*, the β (*C*)- and γ (*D*)-secretase activities did not increase in the brains of *Ttpa*$^{-/-}$ mice compared with wild-type mice.

Aβ Aggregation Study

Five 15-month-old *Ttpa*$^{-/-}$ mice and 10 age-matched wild-type mice were examined. Synaptosomes were prepared from mouse cerebrums as previously reported (22). Seed-free solutions of $A\beta_{1-40}$ were diluted with TBS. Aβ solutions at 50 μM were incubated at 37 °C with or without synaptosomes. Thioflavin T fluorescence intensities in the mixture incubated for 24 h were determined as previously described (23, 24).

Data Analysis

All data represent the average ± S.E. For multiple comparisons, single-factor analysis of variance followed by Fisher's protected least-significant-difference post hoc test was used. Results were considered statistically significant at $p < 0.05$.

RESULTS

Ttpa$^{-/-}$*APPsw Mouse Has an Enhanced Accumulation of Aβ in the Brain*—First, we biochemically studied the effect of α-Toc depletion on accumulation of Aβ. At 18 months, *Ttpa*$^{-/-}$*APPsw* mice showed markedly increased levels of $A\beta_{1-40}$ in the TBS-insoluble fraction of the brain homogenate and a similar tendency of increase of $A\beta_{1-40}$ and $A\beta_{1-42}$ in other fractions (Fig. 1, *A* and *B*). The *in vivo* accumulation of $A\beta_{1-40}$ was decreased when *Ttpa*$^{-/-}$*APPsw* mice were fed on the α-Toc-supplemented diet (Fig. 1*A*). An incomplete effect of α-Toc supplementation on accumulation of Aβ might be explained by the poor recruitment of supplemented α-Toc into the brain in *Ttpa*$^{-/-}$*APPsw* mice, because α-TTP in the brain transports α-Toc from blood to brain (7). This partial effect of α-Toc supplementation still could reduce accumulation of Aβ plaques (12).

APP Expression and β/γ Cleavages Are Not Increased—To examine the effect of α-Toc depletion on the metabolism of Aβ, we evaluated Aβ generation by measuring APP expression and secretase activities. The mRNA level of human APPsw in the brain did not increase in the brains of *Ttpa*$^{-/-}$*APPsw* mice compared with *APPsw* mice at 18 months of age (Fig. 2*A*). Moreover, protein levels of C-terminal fragments of APP-β, -α, and -γ/ε did not change in the brains of *Ttpa*$^{-/-}$*APPsw* mice compared with *APPsw* mice (Fig. 2*B*). This was supported by the *in vitro* results that β- and γ-secretase activities were not increased in the brains of 9-month-old *Ttpa*$^{-/-}$ mice (Fig. 2, *C* and *D*). These results indicate that the generation of Aβ in the brain of *Ttpa*$^{-/-}$*APPsw* mouse is not influenced by the depletion of α-Toc.

Aβ Clearance from the Brain Is Decreased in Ttpa$^{-/-}$ *Mice*—The increased Aβ accumulation without change of Aβ generation in *Ttpa*$^{-/-}$*APPsw* mouse brain led us to postulate that the increased Aβ accumulation by lipid peroxidation occurs through decreased Aβ clearance from the brain. Then we next directly studied Aβ clearance from the brain *in vivo* by using the BEI method (16, 17). We used *Ttpa*$^{-/-}$ mice in this experiment, because the injected ^{125}I-$A\beta_{1-40}$ should have been competed with endogenous Aβ, which accumulated in different degree in *Ttpa*$^{-/-}$*APPsw* and *APPsw* mouse brains, thereby complicating interpretation of the results. In contrast, *Ttpa*$^{-/-}$ mice have no detectable endogenous mouse Aβ in the brain. The ^{125}I-$A\beta_{1-40}$ was microinjected into the mouse cerebral cortex, and the remaining ^{125}I-$A\beta_{1-40}$ levels in the ipsilateral cerebrum were measured. The percentage of ^{125}I-$A\beta_{1-40}$ remaining at 60 min after injection was increased in 14-month-old *Ttpa*$^{-/-}$ mice compared with age-matched wild-type mice (Fig. 3*A*). The apparent elimination rate constant (k_e) was also markedly decreased because of α-Toc depletion (Fig. 3*B*). Although Aβ clearance decreases as a consequence of normal aging (25, 26), the reduction in k_e value evoked by α-Toc depletion (27.7%) was

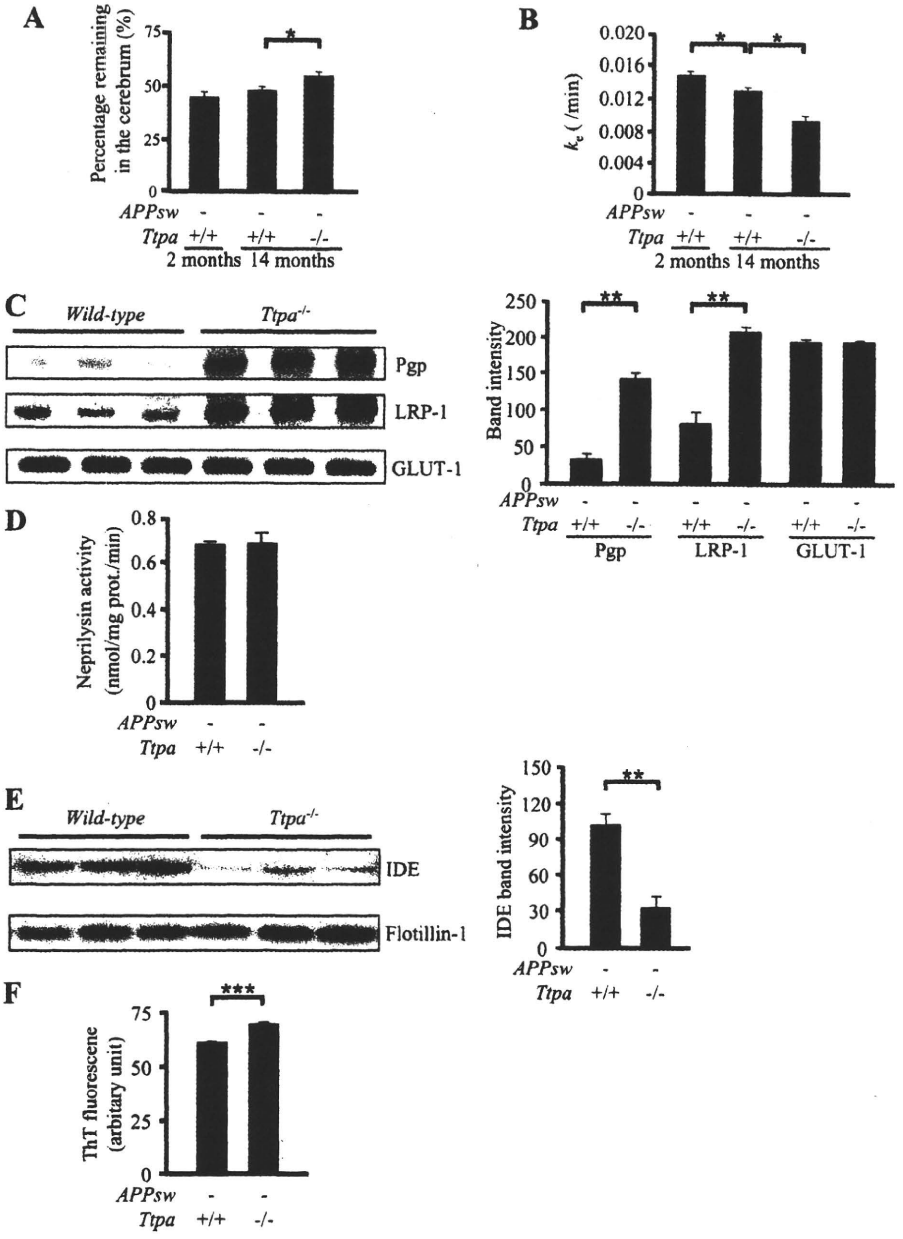

FIGURE 3. **α-Toc depletion decreases Aβ clearance.** *A*, the remaining percentage of ^{125}I-Aβ_{1-40} at 60 min was higher in 14-month-old *Ttpa*$^{-/-}$ mice than in age-matched wild-type mice. *B*, k_e was markedly decreased in *Ttpa*$^{-/-}$ mice. *C*, protein levels of LRP-1 and Pgp were increased in the brains of *Ttpa*$^{-/-}$ mice compared with wild-type mice, whereas levels of GLUT-1 were not changed between them. Band intensities are shown in the *right panel*. *D*, neprilysin-dependent endopeptidase activity did not decrease in *Ttpa*$^{-/-}$ mice compared with wild-type mice. *E*, protein levels of IDE were decreased in the brains of *Ttpa*$^{-/-}$ mice compared with wild-type mice. Band intensities are shown in the *right panel*. *F*, thioflavin T (*ThT*) fluorescence intensity in the incubation mixtures of synaptosomes with synthetic Aβ_{1-40} was increased in the brains of *Ttpa*$^{-/-}$ mice compared with wild-type mice. *, $p < 0.05$; **, $p < 0.01$; ***, $p < 0.0001$.

much greater than that by aging, as shown between 2 and 14 months of age (13.4%). One of the most likely pathologies influencing Aβ clearance is the compromised BBB by oxidative stress with vitamin E deficiency. However, there is no evidence of abnormal structures of endothelial cells or ischemic change on histological analysis of the *Ttpa*$^{-/-}$ mouse brains (data not shown).

Efflux Transporters for Aβ across the BBB Are Up-regulated in the Brain Capillary Endothelial Cells of Ttpa$^{-/-}$ *Mouse*—One of possible causes of impaired Aβ clearance is the decreased efflux and the decreased degradation of Aβ. To examine whether reported molecules involved in Aβ transport at the BBB were down-regulated, we measured the protein levels of LRP-1 and Pgp. Surprisingly, both protein levels in the small vascular fraction in the brains of *Ttpa*$^{-/-}$ mice were much increased compared with wild-type mice (Fig. 3*C*). In contrast, there was no change in the levels of GLUT-1, which is a transporter localized to the brain capillary endothelial cells (27).

Aβ-degrading Peptidase, IDE, Is Decreased in Ttpa$^{-/-}$ *Mouse Brain*—Next, we studied Aβ-degrading peptidases, neprilysin and IDE, for studying another possible cause of impaired Aβ clearance. Although the enzymatic activity of neprilysin was not decreased in *Ttpa*$^{-/-}$ mouse brain compared with wild-type mouse (Fig. 3*D*), expression level of IDE was markedly decreased in *Ttpa*$^{-/-}$ mouse brain (Fig. 3*E*). We, therefore, consider that an impaired degradation of Aβ in the brain because of decreased IDE is related with enhanced Aβ accumulation in *Ttpa*$^{-/-}$*APPsw* mouse brain.

Aβ Aggregation Is Accelerated in Ttpa$^{-/-}$ *Mouse Brains*—Moreover, we studied the effect of oxidative stress on Aβ aggregation capacity. The aggregation of Aβ_{1-40} in the presence of synaptosomes was measured by using thioflavin T fluorescence. The aggregation capacity was increased in brain homogenates of the *Ttpa*$^{-/-}$ mice compared with wild-type homogenates (Fig. 3*F*).

Ttpa$^{-/-}$*APPsw Mouse Has an Increased Level of Aβ in the Plasma as Well as in the Brain*—Furthermore, we measured the plasma levels of Aβ in *Ttpa*$^{-/-}$*APPsw* mouse. The 18-month-old *Ttpa*$^{-/-}$*APPsw* mice showed markedly increased levels of both plasma Aβ_{1-40} and Aβ_{1-42} (Fig. 4*A*). These accumulations of Aβ_{1-40} and Aβ_{1-42} were partially recovered when *Ttpa*$^{-/-}$*APPsw* mice were fed on the α-Toc-supplemented diet (Fig. 4*A*). In contrast, the Aβ-binding proteins in the plasma,

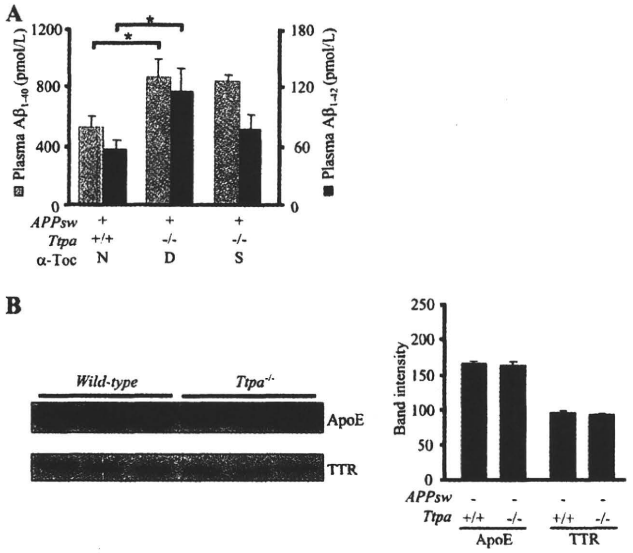

FIGURE 4. **The *Ttpa*$^{-/-}$*APPsw* mouse shows enhanced accumulation of Aβ in the plasma.** *A*, 18-month-old *Ttpa*$^{-/-}$*APPsw* mice showed increased levels of $A\beta_{1-40}$ and $A\beta_{1-42}$. This increase was partially ameliorated by α-Toc supplementation in the diet. *B*, protein levels of apoE and TTR were not changed in the plasma of *Ttpa*$^{-/-}$ mice compared with wild-type mice. Band intensities are shown in the *right panel*. *D*, α-Toc-deficient diet; *S*, α-Toc-supplemented diet; *N*, normal diet. *, $p < 0.05$.

apoE, and TTR levels were not different between *Ttpa*$^{-/-}$ mice and wild-type mice (Fig. 4*B*).

Increased Aβ Accumulation in the Plasma Is also Caused by Impairment of Aβ Clearance from the Blood—The systemic clearance of Aβ should influence the levels of plasma Aβ. Therefore, the effect of *Ttpa* deficiency on systemic clearance of Aβ from the circulation was investigated *in vivo*. We also used *Ttpa*$^{-/-}$ in this experiment instead of *Ttpa*$^{-/-}$*APPsw* and *APPsw* mice, because the CLtot, a primary pharmacokinetic parameter that is a measure of the elimination efficiency of peripherally injected ^{125}I-$A\beta_{1-40}$, is known to decrease significantly in the presence of high plasma levels of $A\beta_{1-40}$ (28). Fig. 5*A* shows the plasma concentration-time profiles of trichloroacetic acid-precipitable ^{125}I-$A\beta_{1-40}$ after intravenous bolus administration in 2- and 25-month-old wild-type and 25-month-old *Ttpa*$^{-/-}$ mice. Plasma concentration of trichloroacetic acid-precipitable ^{125}I-$A\beta_{1-40}$ in 25-month-old *Ttpa*$^{-/-}$ mice was significantly greater at 1, 3, 60, and 360 min and substantially greater at all time points than that in 25-month-old wild-type mice (supplemental Table 1). As shown in supplemental Table 2, the AUC for *Ttpa*$^{-/-}$ mice was significantly greater than that for age-matched wild-type mice by 2.8-fold. To evaluate the systemic clearance more in detail, other pharmacokinetic parameters were determined and summarized in supplemental Table 2. In 25-month-old *Ttpa*$^{-/-}$ mice, CLtot and k_e (elimination rate constant) were significantly decreased by 41.2 and 51.7%, respectively, compared with those in age-matched wild-type mice (Fig. 5*B* and supplemental Table 2). The reduction in CLtot evoked by α-Toc depletion (41.2%) was much greater than that by aging, as shown between 2 and 25 months of age (14.1%) in model-independent moment analysis. The similar results were obtained in model dependent analysis as well (supplemental Table 2).

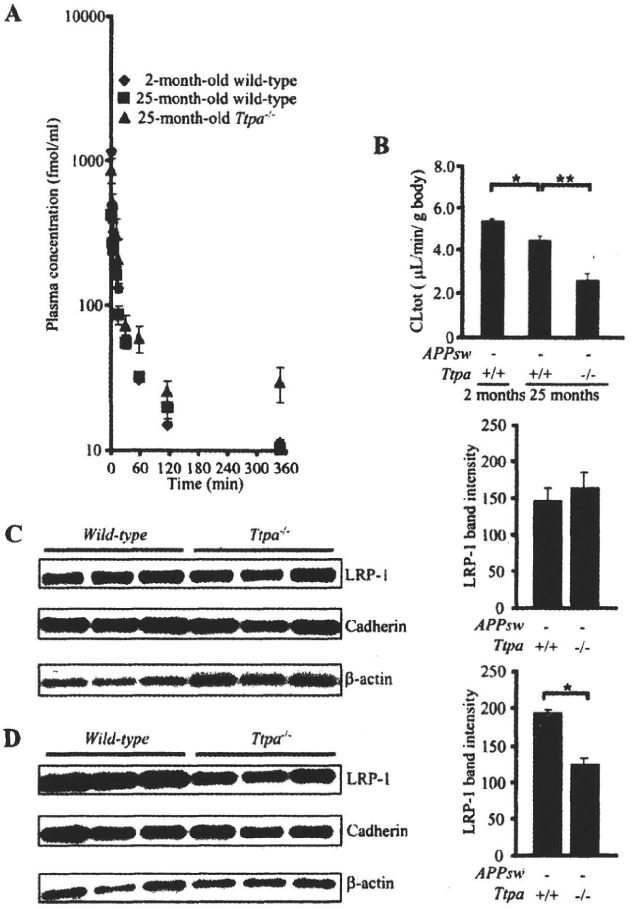

FIGURE 5. **α-Toc depletion decreases Aβ clearance from the plasma.** *A*, the remaining level of trichloroacetic acid-precipitable ^{125}I-$A\beta_{1-40}$ after its injection from the jugular vein was higher in 25-month-old *Ttpa*$^{-/-}$ mice than in wild-type mice. *B*, the total body clearance of ^{125}I-$A\beta_{1-40}$ was markedly decreased in *Ttpa*$^{-/-}$ mice compared with wild-type mice. *C* and *D*, the protein level of LRP-1 was decreased not in the crude membrane fraction of the liver of *Ttpa*$^{-/-}$ mice (*C*) but in the plasma membrane fraction (*D*) compared with wild-type mice. *, $p < 0.05$.

These results demonstrated that systemic clearance was attenuated in 25-month-old *Ttpa*$^{-/-}$ mice, and the decrease in the systemic clearance is likely to be because of a decrease in the clearance from the liver, as the systemic clearance of Aβ has been reported to be mostly mediated by clearance from the liver (29, 30).

LRP-1 Is Down-regulated in the Plasma Membrane Fraction of the Liver in Ttpa$^{-/-}$ *Mice*—To examine whether the Aβ receptor was down-regulated in the liver for the cause of impaired Aβ clearance from the blood, we measured the protein level of LRP-1 in the crude and plasma membrane fractions of the liver, as LRP-1 translocates from Golgi apparatus to plasma membrane in their activation for transporting Aβ into the hepatocytes (31). The protein level of LRP-1 was unchanged in the crude membrane fraction but decreased in the plasma membrane fraction of *Ttpa*$^{-/-}$ mouse liver (Fig. 5, *C* and *D*). This inactivation of LRP-1 might explain the decreased clearance of Aβ from the blood, causing increased Aβ in *Ttpa*$^{-/-}$*APPsw* mouse plasma.

DISCUSSION

We clearly demonstrated that Aβ clearances from the brain and from the blood were decreased in *Ttpa*$^{-/-}$ mice. Because the Aβ generation in *Ttpa*$^{-/-}$*APPsw* mouse brain was not increased, we consider that accumulated Aβ in *Ttpa*$^{-/-}$*APPsw* mouse brain is caused by these impaired Aβ clearances. The Aβ clearance from the brain can be accomplished via two major pathways; that is, receptor-mediated transport from the brain and proteolytic degradation in the brain. First, two proteins expressed in brain endothelial cells, LRP-1 and Pgp, are reported to regulate Aβ clearance by controlling its efflux from brain to blood based on the studies of genetically engineered mice (32, 33). Actually, LRP-1 was down-regulated in older mice, and this down-regulation correlated with Aβ accumulation in AD brains (25). Pgp expression was also inversely correlated with deposition of Aβ in the brains of elderly non-demented humans (34). Surprisingly, both LRP-1 and Pgp levels are markedly increased in *Ttpa*$^{-/-}$ mouse brains, although clearance of ^{125}I-Aβ$_{1-40}$ by the BEI method is impaired. There are two possible explanations for the up-regulations of LRP-1 and Pgp. One is to compensate their dysfunctions, and another is to transport increased other substrates in the brain caused by lipid peroxidation. Second, the two major endopeptidases involved in proteolysis-related degradation of Aβ in the brain are neprilysin and IDE. Whereas the activity of neprilysin was not decreased, the protein level of IDE was markedly decreased in *Ttpa*$^{-/-}$ mouse brain. Furthermore, we made a gene chip analysis and evaluated all the molecules cyclopedically in the brains of *Ttpa*$^{-/-}$ and wild-type littermate mice. As a result, the only reasonable change of expression level for possibly causing enhanced Aβ accumulation was the decrease in IDE mRNA (supplemental Table 3, *A* and *B*). The homozygous deletion of IDE gene are known to show decreased Aβ degradation and increased accumulation of endogenous Aβ in the mouse brains (35, 36). Moreover, we previously confirmed that contribution of IDE to the clearance of microinjected ^{125}I-Aβ$_{1-40}$ in the BEI method could be 25.3% by the pre-administration of IDE inhibitors, bacitracin (26). Together, as one of molecular mechanisms of Aβ accumulation and impaired clearance of Aβ in *Ttpa*$^{-/-}$*APPsw* mouse brains, we think that degradation of Aβ was impaired by decreased expression of IDE. However, we cannot exclude the possibility of dysfunction of other proteins because of lipid peroxidation, which may contribute to abnormal Aβ metabolism.

There are reports that AD patients showed increased levels of peripherally circulating Aβ (37, 38). In *Ttpa*$^{-/-}$*APPsw* mice as well, plasma Aβ levels are proved to be markedly increased to be compared with *APPsw* mice. Significantly lowered clearance of injected ^{125}I-Aβ$_{1-40}$ from the *Ttpa*$^{-/-}$ mouse blood could explain the increased plasma Aβ in *Ttpa*$^{-/-}$*APPsw* mice. Although the excretion of Aβ through the kidney accounts only for a minute portion of Aβ in the blood (39), the liver is the major organ responsible for blood clearance of Aβ (29). We previously reported that LRP-1 in hepatocytes plays an important role to uptake plasma Aβ because mice with down-regulated LRP-1 by knock-out of receptor-associated protein or hydrodynamic injection of siRNA showed a much decreased uptake of ^{125}I-Aβ$_{1-40}$ into the liver (40). The 85-kDa LRP-1 is proteolytically cleaved from a 600-kDa precursor in Golgi apparatus and is translocated by receptor-associated protein to plasma membrane to be activated for bounding Aβ (41). The result of decreased LRP-1 in the plasma membrane fraction without change of LRP-1 level in the crude membrane fraction of *Ttpa*$^{-/-}$ mouse liver indicated that lipid peroxidation does not affect LRP-1 expression itself but suggested a disturbed translocation of LRP-1. In another view, plasma Aβ level could be influenced by a change of its plasma ligands; apoE, TTR, and soluble LRP-1 (30, 42, 43). When soluble LRP-1 is oxidized, it is known to be decreased in its affinity to Aβ$_{1-40}$ and Aβ$_{1-42}$ (43). Although serum apoE and TTR levels in *Ttpa*$^{-/-}$ mice were not decreased, we could not evaluate serum soluble LRP-1 nor oxidized soluble LRP-1 level. Therefore, we cannot exclude the possibility that soluble LRP-1 is affected by the lipid peroxidation and causes the increased Aβ accumulation in *Ttpa*$^{-/-}$*APPsw* mouse plasma.

Given the fact that a large number of sporadic AD cannot be explained by increased Aβ generation (3), better understanding of the molecular and genetic basis of the Aβ clearance mechanisms may hold at least in part the key for research of AD pathology. A strongest risk factor for AD is aging (44), and lipid peroxidation may be a major cause for aging of the brain (45). In these respects, our findings of increased accumulation and aggregation of Aβ with impaired clearance due to lipid peroxidation are new aspects of AD pathology. We hope that further investigation on the molecular mechanism of impaired Aβ clearance due to lipid peroxidation provides a novel diagnostic and therapeutic target of AD.

Acknowledgments—We thank Hiroyuki Arai, Mikio Shoji, Akihiko Nunomura, and Masaki Nishimura for invaluable suggestions and discussion and Iichirou Oonishi for assistance.

REFERENCES

1. Li, R., Lindholm, K., Yang, L. B., Yue, X., Citron, M., Yan, R., Beach, T., Sue, L., Sabbagh, M., Cai, H., Wong, P., Price, D., and Shen, Y. (2004) *Proc. Natl. Acad. Sci. U.S.A.* **101,** 3632–3637
2. Iwata, N., Higuchi, M., and Saido, T. C. (2005) *Pharmacol. Ther.* **108,** 129–148
3. Zlokovic, B. V. (2004) *J. Neurochem.* **89,** 807–811
4. Barnham, K. J., Masters, C. L., and Bush, A. I. (2004) *Nat. Rev. Drug Discov.* **3,** 205–214
5. Moreira, P. I., Smith, M. A., Zhu, X., Nunomura, A., Castellani, R. J., and Perry, G. (2005) *Ann. N.Y. Acad. Sci.* **1043,** 545–552
6. Andersen, J. K. (2004) *Nat. Med.* **10,** S18–25
7. Yokota, T., Igarashi, K., Uchihara, T., Jishage, K., Tomita, H., Inaba, A., Li, Y., Arita, M., Suzuki, H., Mizusawa, H., and Arai, H. (2001) *Proc. Natl. Acad. Sci. U.S.A.* **98,** 15185–15190
8. Traber, M. G., Burton, G. W., and Hamilton, R. L. (2004) *Ann. N.Y. Acad. Sci.* **1031,** 1–12
9. Dowson, J. H., Mountjoy, C. Q., Cairns, M. R., and Wilton-Cox, H. (1992) *Neurobiol Aging* **13,** 493–500
10. Lovell, M. A., Ehmann, W. D., Butler, S. M., and Markesbery, W. R. (1995) *Neurology* **45,** 1594–1601
11. Sayre, L. M., Zelasko, D. A., Harris, P. L., Perry, G., Salomon, R. G., and Smith, M. A. (1997) *J. Neurochem.* **68,** 2092–2097
12. Nishida, Y., Yokota, T., Takahashi, T., Uchihara, T., Jishage, K., and Mizusawa, H. (2006) *Biochem. Biophys. Res. Commun.* **350,** 530–536
13. Hsiao, K., Chapman, P., Nilsen, S., Eckman, C., Harigaya, Y., Younkin, S.,

Yang, F., and Cole, G. (1996) *Science* **274,** 99–102
14. Kanda, T., Yoshino, H., Ariga, T., Yamawaki, M., and Yu, R. K. (1994) *J. Cell Biol.* **126,** 235–246
15. Apelt, J., Bigl, M., Wunderlich, P., and Schliebs, R. (2004) *Int. J. Dev. Neurosci.* **22,** 475–484
16. Kakee, A., Terasaki, T., and Sugiyama, Y. (1996) *J. Pharmacol. Exp. Ther.* **277,** 1550–1559
17. Hino, T., Yokota, T., Ito, S., Nishina, K., Kang, Y. S., Mori, S., Hori, S., Kanda, T., Terasaki, T., and Mizusawa, H. (2006) *Biochem. Biophys. Res. Commun.* **340,** 263–267
18. Yamaoka, K., Tanigawara, Y., Nakagawa, T., and Uno, T. (1981) *J. Pharmacobiodyn.* **4,** 879–885
19. Tabata, K., Yamaoka, K., Kaibara, A., Suzuki, S., Terakawa, M., and Hata, T. (1999) *Xenobiol. Metabol. Dispos.* **14,** 286–293
20. Yamaoka, K., Nakagawa, T., and Uno, T. (1978) *J. Pharmacokinet. Biopharm.* **6,** 547–558
21. Ogawa, T., Kiryu-Seo, S., Tanaka, M., Konishi, H., Iwata, N., Saido, T., Watanabe, Y., and Kiyama, H. (2005) *J. Neurochem.* **95,** 1156–1166
22. Igbavboa, U., Avdulov, N. A., Schroeder, F., and Wood, W. G. (1996) *J. Neurochem.* **66,** 1717–1725
23. Naiki, H., and Gejyo, F. (1999) *Methods Enzymol.* **309,** 305–318
24. Hayashi, H., Kimura, N., Yamaguchi, H., Hasegawa, K., Yokoseki, T., Shibata, M., Yamamoto, N., Michikawa, M., Yoshikawa, Y., Terao, K., Matsuzaki, K., Lemere, C. A., Selkoe, D. J., Naiki, H., and Yanagisawa, K. (2004) *J. Neurosci.* **24,** 4894–4902
25. Shibata, M., Yamada, S., Kumar, S. R., Calero, M., Bading, J., Frangione, B., Holtzman, D. M., Miller, C. A., Strickland, D. K., Ghiso, J., and Zlokovic, B. V. (2000) *J. Clin. Invest.* **106,** 1489–1499
26. Shiiki, T., Ohtsuki, S., Kurihara, A., Naganuma, H., Nishimura, K., Tachikawa, M., Hosoya, K., and Terasaki, T. (2004) *J. Neurosci.* **24,** 9632–9637
27. Pardridge, W. M., Boado, R. J., and Farrell, C. R. (1990) *J. Biol. Chem.* **265,** 18035–18040
28. Kandimalla, K. K., Curran, G. L., Holasek, S. S., Gilles, E. J., Wengenack, T. M., and Poduslo, J. F. (2005) *J. Pharmacol. Exp. Ther.* **313,** 1370–1378
29. Ghiso, J., Shayo, M., Calero, M., Ng, D., Tomidokoro, Y., Gandy, S., Rostagno, A., and Frangione, B. (2004) *J. Biol. Chem.* **279,** 45897–45908
30. Hone, E., Martins, I. J., Fonte, J., and Martins, R. N. (2003) *J. Alzheimers Dis.* **5,** 1–8
31. Tamaki, C., Ohtsuki, S., and Terasaki, T. (2007) *Mol. Pharmacol.* **72,** 850–855
32. Van, Uden, E., Mallory, M., Veinbergs, I., Alford, M., Rockenstein, E., and Masliah, E. (2002) *J. Neurosci.* **22,** 9298–9304
33. Cirrito, J. R., Deane, R., Fagan, A. M., Spinner, M. L., Parsadanian, M., Finn, M. B., Jiang, H., Prior, J. L., Sagare, A., Bales, K. R., Paul, S. M., Zlokovic, B. V., Piwnica-Worms, D., and Holtzman, D. M. (2005) *J. Clin. Invest.* **115,** 3285–3290
34. Vogelgesang, S., Cascorbi, I., Schroeder, E., Pahnke, J., Kroemer, H. K., Siegmund, W., Kunert-Keil, C., Walker, L. C., and Warzok, R. W. (2002) *Pharmacogenetics* **12,** 535–541
35. Farris, W., Mansourian, S., Chang, Y., Lindsley, L., Eckman, E. A., Frosch, M. P., Eckman, C. B., Tanzi, R. E., Selkoe, D. J., and Guenette, S. (2003) *Proc. Natl. Acad. Sci. U.S.A.* **100,** 4162–4167
36. Miller, B. C., Eckman, E. A., Sambamurti, K., Dobbs, N., Chow, K. M., Eckman, C. B., Hersh, L. B., and Thiele, D. L. (2003) *Proc. Natl. Acad. Sci. U.S.A.* **100,** 6221–6226
37. Kuo, Y. M., Emmerling, M. R., Lampert, H. C., Hempelman, S. R., Kokjohn, T. A., Woods, A. S., Cotter, R. J., and Roher, A. E. (1999) *Biochem. Biophys. Res. Commun.* **257,** 787–791
38. Matsubara, E., Ghiso, J., Frangione, B., Amari, M., Tomidokoro, Y., Ikeda, Y., Harigaya, Y., Okamoto, K., and Shoji, M. (1999) *Ann. Neurol.* **45,** 537–541
39. Ghiso, J., Calero, M., Matsubara, E., Governale, S., Chuba, J., Beavis, R., Wisniewski, T., and Frangione, B. (1997) *FEBS Lett.* **408,** 105–108
40. Tamaki, C., Ohtsuki, S., Iwatsubo, T., Hashimoto, T., Yamada, K., Yabuki, C., and Terasaki, T. (2006) *Pharm. Res.* **23,** 1407–1416
41. Willnow, T. E., Armstrong, S. A., Hammer, R. E., and Herz, J. (1995) *Proc. Natl. Acad. Sci. U.S.A.* **92,** 4537–4541
42. Matsubara, E., Sekijima, Y., Tokuda, T., Urakami, K., Amari, M., Shizuka-Ikeda, M., Tomidokoro, Y., Ikeda, M., Kawarabayashi, T., Harigaya, Y., Ikeda, S., Murakami, T., Abe, K., Otomo, E., Hirai, S., Frangione, B., Ghiso, J., and Shoji, M. (2004) *Neurobiol. Aging* **25,** 833–841
43. Sagare, A., Deane, R., Bell, R. D., Johnson, B., Hamm, K., Pendu, R., Marky, A., Lenting, P. J., Wu, Z., Zarcone, T., Goate, A., Mayo, K., Perlmutter, D., Coma, M., Zhong, Z., and Zlokovic, B. V. (2007) *Nat. Med.* **13,** 1029–1031
44. Katzman, R., and Saitoh, T. (1991) *FASEB J.* **5,** 278–286
45. Sohal, R. S., and Weindruch, R. (1996) *Science* **273,** 59–63

THE JOURNAL OF BIOLOGICAL CHEMISTRY VOL. 283, NO. 28, pp. 19489–19498, July 11, 2008

Evidence That CD147 Modulation of β-Amyloid (Aβ) Levels Is Mediated by Extracellular Degradation of Secreted Aβ*◆

Received for publication, February 7, 2008, and in revised form, April 30, 2008 Published, JBC Papers in Press, May 1, 2008, DOI 10.1074/jbc.M801037200

Kulandaivelu S. Vetrivel[‡1], Xulun Zhang[‡1], Xavier Meckler[‡], Haipeng Cheng[‡], Sungho Lee[‡], Ping Gong[‡], Kryslaine O. Lopes[‡], Ying Chen[‡], Nobuhisa Iwata[§], Ke-Jie Yin[¶], Jin-Moo Lee[¶], Angèle T. Parent[‡], Takaomi C. Saido[§], Yue-Ming Li[‖], Sangram S. Sisodia[‡2], and Gopal Thinakaran[‡3]

From the [‡]Departments of Neurobiology and Neurology, The University of Chicago, Chicago, Illinois 60637, the [§]Laboratory for Proteolytic Neuroscience, RIKEN Brain Science Institute, 2-1 Hirosawa, Wako-shi, Saitama 351-0198, Japan, the [¶]Department of Neurology and the Hope Center for Neurological Disorders, Washington University School of Medicine, St. Louis, Missouri 63110, and the [‖]Molecular Pharmacology and Chemistry Program, Memorial Sloan-Kettering Cancer Center, New York, New York 10021

Cerebral deposition of β-amyloid (Aβ) peptides is a pathological hallmark of Alzheimer disease. Intramembranous proteolysis of amyloid precursor protein by a multiprotein γ-secretase complex generates Aβ. Previously, it was reported that CD147, a glycoprotein that stimulates production of matrix metalloproteinases (MMPs), is a subunit of γ-secretase and that the levels of secreted Aβ inversely correlate with CD147 expression. Here, we show that the levels and localization of CD147 in fibroblasts, as well as postnatal expression and distribution in brain, are distinct from those of integral γ-secretase subunits. Notably, we show that although depletion of CD147 increased extracellular Aβ levels in intact cells, membranes isolated from CD147-depleted cells failed to elevate Aβ production in an *in vitro* γ-secretase assay. Consistent with an extracellular source that modulates Aβ metabolism, synthetic Aβ was degraded more rapidly in the conditioned medium of cells overexpressing CD147. Moreover, modulation of CD147 expression had no effect on ε-site cleavage of amyloid precursor protein and Notch1 receptor. Collectively, our results demonstrate that CD147 modulates Aβ levels not by regulating γ-secretase activity, but by stimulating extracellular degradation of Aβ. In view of the known function of CD147 in MMP production, we postulate that CD147 expression influences Aβ levels by an indirect mechanism involving MMPs that can degrade extracellular Aβ.

Alzheimer disease is an age-associated neurodegenerative disorder that is clinically manifested by the progressive loss of memory and cognitive functions. An early event in the development of Alzheimer disease is the aggregation and deposition of β-amyloid (Aβ)[4] peptides in the brains of affected individuals. Aβ is derived from type I transmembrane protein, termed amyloid precursor protein (APP), through sequential cleavage by β- and γ-secretases (1, 2). γ-Secretase is a multimeric protein complex consisting of presenilin (PS1 or PS2), nicastrin, APH1, and PEN-2 as core subunits (2). The exact functional contribution of each γ-secretase subunit to enzyme activity has not been fully elucidated, but multiple lines of evidence suggest that PS1, a protein that accumulates as endoproteolytically processed N-terminal (NTF) and C-terminal (CTF) fragments, is the catalytic center of γ-secretase, whereas nicastrin appears to facilitate substrate recruitment (3–5). Coexpression of these four transmembrane proteins is sufficient to reconstitute γ-secretase activity in yeast, an organism that lacks orthologous proteins (6). Gene knock-out and small interfering RNA (siRNA)-mediated knockdown studies have demonstrated that Aβ production is compromised in the absence of any one of these core components (7–10). Collectively, these latter studies establish that PS1, nicastrin, APH1, and PEN-2 are necessary and sufficient for γ-secretase processing of APP.

The biogenesis, maturation, stability, and steady-state levels of γ-secretase complex subunits are codependent (reviewed in Ref. 11). For example, limiting expression of any one of the integral components affects the post-translational maturation and stability of the other subunits, indicating that their assembly into high molecular mass complexes is a highly regulated process that occurs during biosynthesis of these polypeptides. In this regard, the heavily glycosylated type I membrane protein nicastrin does not mature and exit the endoplasmic reticulum (ER) in cells lacking PS1 expression (12). On the other hand, PS1 fails to undergo endoproteolysis to generate stable NTFs

* This work was supported, in whole or in part, by National Institutes of Health Grants AG021495 and AG019070 (to G. T.) and AG026660 (to Y.-M. L.). This work was also supported by Grants-in-aid for Scientific Research on Priority Areas 17025046 and 18023037 from the Ministry of Education, Culture, Sports, Science, and Technology of Japan (to N. I.), by an Alzheimer's Association investigator-initiated research grant (to G. T.) and new investigator research grant (to K. S. V.), and by grants from the American Health Assistance Foundation (to G. T. and S. S. S.). The costs of publication of this article were defrayed in part by the payment of page charges. This article must therefore be hereby marked "*advertisement*" in accordance with 18 U.S.C. Section 1734 solely to indicate this fact.
◆ This article was selected as a Paper of the Week.
[1] Both authors contributed equally to this work.
[2] To whom correspondence may be addressed: Dept. of Neurobiology, The University of Chicago, Abbott 308, 947 E. 58th Street, Chicago, IL 60637. Tel.: 773-834-9186; Fax: 773-702-2926; E-mail: ssisodia@bsd.uchicago.edu.
[3] To whom correspondence may be addressed: Dept. of Neurobiology, The University of Chicago, Knapp R212, 924 E. 57th St., Chicago, IL 60637. Tel.: 773-834-3752; Fax: 773-834-3808; E-mail: gopal@uchicago.edu.

[4] The abbreviations used are: Aβ, β-amyloid; APP, amyloid precursor protein; PS, presenilin; NTF, N-terminal fragment; CTF, C-terminal fragment; siRNA, small interfering RNA; ER, endoplasmic reticulum; MMP, matrix metalloproteinase; MEFs, mouse embryonic fibroblasts; CHAPSO, 3-[(3-cholamidopropyl)dimethylammonio]-2-hydroxy-1-propanesulfonic acid; DRM, detergent-resistant membrane; MOPS, 4-morpholinepropanesulfonic acid; ELISA, enzyme-linked immunosorbent assay; WT, wild-type; AICD, APP intracellular domain; NICD, Notch intracellular domain; Tricine, *N*-[2-hydroxy-1,1-bis(hydroxymethyl)ethyl]glycine.

and CTFs in cells lacking nicastrin, APH1a, or PEN-2 expression (11). The use of detergents with dissimilar solubilization properties and different biochemical purification methods has led to discrepant size predictions of the active γ-secretase complexes, with estimates ranging from 250 kDa to 2 MDa (13, 14). Although a recent study has shown that active γ-secretase contains one of each of these four essential components (15), it is notable that the estimated sizes of the γ-secretase complexes exceed the sum of the four integral subunits. Thus, it is generally anticipated that one or more cofactors might associate with the four integral subunits of the γ-secretase complex and that these polypeptides modulate enzyme activity.

Recently, two type I membrane proteins, CD147 and p23, have been shown to co-immunoisolate with the γ-secretase complex and regulate Aβ levels (16, 17). CD147 (also called EMMPRIN (extracellular matrix metalloproteinase inducer), Basigin, neurothelin, and M6 leukocyte activation antigen) is a multifunctional cell-surface type I transmembrane protein that stimulates matrix metalloproteinase (MMP) secretion (18). p23 (also called TMP21) is a member of the p24 type I transmembrane protein family involved in vesicular trafficking between the ER and Golgi (19). siRNA-mediated knockdown of CD147 or p23 expression causes dose-dependent increases in the levels of secreted Aβ (16, 17). Nevertheless, because only a small fraction of the cellular pool of CD147 or p23 remains complexed with γ-secretase at steady state, the precise mechanisms by which these proteins modulate γ-secretase activity remain obscure. For example, p23 influences Aβ levels by modulating γ-secretase cleavage of APP and by regulating secretory trafficking of APP and possibly APP secretases (20). In this study, we show that CD147 does not directly modulate γ-secretase cleavage of APP substrate in an *in vitro* γ-secretase assay. Instead, we found evidence for enhanced degradation of Aβ in medium conditioned by cells overexpressing CD147, suggesting the potential involvement of CD147-induced MMP secreted forms in modulating extracellular Aβ levels. Consistent with this indirect mechanism, the absence of PS1 and nicastrin has no effect on CD147 stability and subcellular localization, and CD147 expression fails to influence γ-secretase subunit expression and lipid raft association. A distinct expression pattern and distribution of CD147 and nicastrin in brain further support our view that CD147 regulates extracellular Aβ levels via mechanisms independent of γ-secretase processing of APP.

EXPERIMENTAL PROCEDURES

cDNA Constructs and Oligonucleotides—Human CD147 cDNA was generated by reverse transcription-PCR using total RNA isolated from HEK293 cells. C-terminally Myc/His-tagged CD147 was constructed by subcloning CD147 cDNA into the pAG3-Myc-His vector. The following primers were used to generate RNA duplexes using a Silencer siRNA construction kit (Ambion): CD147 siRNA, AAGACCTTGGCTCCAAGATACCCTGTCTC and AAGTATCTTGGAGCCAAGGTCCCTGTCTC; and scrambled siRNA, AACTCTTCCGCGTAGCAAAGACCTGTCTC and AATCTTTGCTACGCGGAAGAGCCTGTCTC. The cDNA encoding C-terminally Myc-tagged APP (APPswe-6Myc) (a kind gift from Dr. Alison Goate) (21) was subcloned into the pCB6 vector. An expression plasmid encoding truncated Notch1 (mNotchΔE) was kindly provided by Dr. Jeffrey S. Nye.

Cell Lines—Mouse embryonic fibroblasts (MEFs) and HEK293 cells were maintained in Dulbecco's modified Eagle's medium supplemented with 10% fetal bovine serum. HEKswe cells were maintained in the presence of 200 μg/ml G418 (22). HEK293 cells were transfected with CD147-Myc-His plasmid, and stable transfectants were selected as pools in the presence of 200 μg/ml Zeocin. $PS1^{-/-}/PS2^{-/-}$ and $NCT^{-/-}$ cells stably expressing PS1 or nicastrin were generated by retroviral infections of MEFs and selected in the presence of 4 μg/ml puromycin as described previously (23). CD147 and scrambled siRNA duplexes were transfected into HEK293 cells using Lipofectamine (Invitrogen) and analyzed after 48 h.

Co-immunoprecipitation—$PS1^{-/-}/PS2^{-/-}$ cells stably expressing either vector or PS1 were lysed in buffer containing 1% CHAPSO, 25 mM HEPES (pH 7.4), 150 mM NaCl, 2 mM EDTA, and a mixture of protease inhibitors. Equal amounts of proteins from the post-nuclear supernatants were used for co-immunoisolation using the $PS1_{NT}$ antibody as described previously (24).

Protein Analysis, Immunostaining, and Detergent-resistant Membrane (DRM) Isolation—Total protein lysates from cultured cells and mouse brain harvested during embryonic and postnatal developmental stages were prepared essentially as described previously (25). Antibodies against γ-secretase subunits, APP, and organelle markers have been described (26). Goat anti-CD147 (Santa Cruz Biotechnology) and anti-human CD147 (Chemicon) monoclonal antibodies were used to detect CD147. Immunofluorescence staining and isolation of DRMs from Lubrol WX lysates of cultured cells by discontinuous flotation density gradients were performed as described (26, 27). Immunohistochemical staining was performed on 30-μm sagittal sections of 2-month-old C57BL/6J mouse brain with rabbit anti-nicastrin (SP718; 1:1000) or goat anti-CD147 (1:5000) antibody as described (28).

In Vitro γ-Secretase Assays—Membranes prepared from HEK293 cells transfected with either scrambled or CD147 siRNA were used to examine γ-secretase activity using C100-FLAG substrate as described previously (14). Briefly, cells were homogenized 10 times using a glass-Teflon homogenizer in buffer containing 10 mM MOPS, 10 mM KCl, 1 mM EDTA, and protease inhibitor mixture. The homogenate was subjected to centrifugation at 1000 × *g* for 10 min at 4 °C. The supernatant was saved, and the pellet was passed through one more round of homogenization. Pooled supernatants were centrifuged at 100,000 × *g* for 1 h at 4 °C. The resulting pellet was resuspended in homogenization buffer and centrifuged again at 100,000 × *g* for 1 h at 4 °C. The pellet-containing membranes were used for *in vitro* γ-secretase activity assay in the presence or absence of 1 μM L685,458 to establish the specificity of the assay.

Aβ Digestion Assay Using Synthetic Aβ—9 μl of culture medium was incubated with 6 ng of synthetic $Aβ_{40}$ or $Aβ_{42}$ for 14 h at 37 °C. After incubation, the reaction mixtures were resolved by gradient SDS-PAGE followed by Western blotting using monoclonal antibody 6E10.